Sediment flow routing during formation of forearc basins: constraints from integrated analysis of detrital pyroxenes and stratigraphy in the Kumano Basin, Japan

Corrected, unformated version for free access. Full edited article available at:
http://doi.org/10.1016/j.epsl.2014.12.046

David M. Buchs (BuchsD@cardiff.ac.uk)
Cardiff University, School of Earth and Ocean Sciences, Main Building, Cardiff, CF10 3AT, United Kingdom / Previous affiliations: (1) GEOMAR- Helmholtz Centre for Ocean Research Kiel, Research Division 4: Dynamics of the Ocean Floor, Wischhofstr. 1-3, 24148 Kiel, Germany; and (2), Research School of Earth Sciences, The Australian National University, ACT 0200 Canberra, Australia

Deniz Cukur
Korea Institute of Geoscience and Mineral Resources (KIGAM), Petroleum and Marine Research Division, 124 Gwahang-no, Yuseong-gu, Daejeon 305-350, KOREA / Previous affiliation: University of Kiel, Institute of Geosciences, Otto Hahn Platz 1, 24118 Kiel, Germany

Hideki Masago
Center for Deep Earth Exploration, Japan Agency for Marine-Earth Science and Technology, 3173‑25 Showa‑machi, Kanazawa‑ku, Yokohama, Kanagawa 236‑0001, Japan

Dieter Garbe-Schönberg
University of Kiel, Institute of Geosciences, Ludewig Meyn Str. 10, 24118 Kiel, Germany

Abstract

The evolution of sediment flow routing during complete evolution of the Kumano forearc basin is determined through integration of stratigraphic and sediment provenance analyses in the upper Nankai forearc. A new approach uses the compositional variability of detrital clinopyroxenes and orthopyroxenes collected at 8 major rivers in Japan and 3 drill sites in the basin and nearby slope environment, including the first drill cuttings retrieved by the Integrated Ocean Drilling Program (IODP). Joint interpretation of these datasets reveals that the sedimentation history of the basin is characterized by three main phases separated by newly-recognised time-transgressive boundaries. We show that the Kumano Basin initiated as a trench-slope basin in the early Quaternary (~1.93 Ma) and that it progressively evolved towards an upper slope environment with increased turbidite confinement and influence from climatic forcing. Basin initiation was broadly synchronous with development of the Nankai megasplay fault, suggesting a causal relationship with construction of the Nankai accretionary prism. Unlike preceding studies documenting long-distance longitudinal transport of clastic material along the lower Nankai forearc, only limited longitudinal transport is documented by detrital pyroxenes in the upper forearc. These results suggest that transverse canyons are a major control on the sediment flow routing during maturation of forearc basins and that long-distance longitudinal flows along convergent margins are principally restricted to near-trench environments, even in the presence of large forearc basins.

Keywords: Kumano forearc basin, turbidity current, pyroxene, drill cuttings, canyon, megasplay fault

1. Introduction

Sediment routing and deposition are important processes at modern convergent margins. The rate and mode of supply of detrital sediments from the volcanic front to the trench are first order controls on formation and development of accretionary complexes and the structural evolution of forearc regions (e.g., Melnick and Echtler, 2006; Kimura et al., 2008; Simpson, 2010). The transport of detrital sediments towards the trench is affected in turn by forearc deformation and development of basins and canyons that control sediment routing in the outer margin (Dickinson and Seely, 1979; Underwood and Karig, 1980; Dicksinson, 1995; Underwood et al., 2003; Underwood and Moore, 2012). In this context, the formation of forearc basins is of particular significance because they form large sediment traps that can profoundly modify the transport and depositional patterns of sediments, with likely implications for the mechanical state of the margin and the formation of earthquakes (Fuller et al., 2006; Wang and Hu, 2006). However, documenting sedimentary patterns during development of these basins has remained limited along modern convergent margins due to a lack of sampling in the deepest parts of mature basins and difficulties in determining the sources of detrital sediments in volcanic environments using common methods of sediment provenance analysis.

The Kumano Basin, located along the Nankai margin, southwest Japan (Fig. 1), offers a unique opportunity to study sediment provenance during different development stages of a forearc basin. Drilling of sedimentary sequences down to the basin basement was recently carried out by deep sea drilling vessel Chikyu at two sites of the Integrated Ocean Drilling Program (IODP) during the Nankai Trough Seismogenic Experiment (NanTroSEIZE) (Kinoshita et al., 2008; Saffer et al., 2010; Strasser et al., 2014). In addition, seismic imaging of the basin and surrounding forearc slope was carried out as preparation to the NanTroSEIZE program (Moore et al., 2009) and during the MITI seismic survey for exploration of methane hydrate in Japan (e.g., Takano et al., 2013). Overall, these operations provide a valuable background to investigate the relationship between tectono-stratigraphic development of the basin and sedimentation patterns in the forearc.

The aim of this paper is to document temporal changes in the sources of detrital sediments deposited in the Kumano Basin and to characterise longitudinal deflection of turbidity currents induced by development of a large sediment trap/accommodation space in the upper forearc. We show this can be achieved through an approach integrating stratigraphic correlation of drilling sites in the basin with sediment provenance analysis based on compositional variations of detrital pyroxenes. In addition, we report on the stratigraphic accuracy of the first IODP cuttings samples, which were retrieved using riser drilling techniques on the Chikyu (Saffer et al., 2010).

2. Geological setting

The Kumano Basin is located along the Nankai margin (Fig. 1), where the Philippine Sea Plate is subducting NW beneath the Eurasian Plate at a rate of ~4.5 cm/y. (Seno et al., 1993). The basin rests in the upper forearc upon a Neogene accretionary prism (Moore et al., 2007; Kinoshita et al., 2008; Saffer et al., 2010; Gulick et al., 2010; Hayman et al. 2012; Takano et al., 2013). It sits between the upper trench slope and a megasplay fault associated with a forearc high that marks the transition downslope to an imbricate thrust zone (Moore et al. 2009; Strasser et al., 2009; Martin et al., 2010). The basin is ~150 km long and ~50 km wide and forms a major bathymetric step at ~2000 m depth between the Honshu shelf (~50 m deep) and the Nankai Trough and Shikoku Basin (~4400 m deep) (Figs 1-2a).

Previous seismic observations and drilling data show that the Kumano Basin started to develop in the early Quaternary and experienced a major phase of landward tilting in the middle Quaternary

Corrected, unformatted version – full edited paper at http://doi.org/10.1016/j.epsl.2014.12.046

(Moore et al., 2007; Gulick et al., 2010; Takano et al., 2013). However, reasons for the basin initiation and subsequent tilting remain unclear. Possible tectonic causes include shortening along the megasplay fault bordering the basin (Moore et al., 2007; Bangs et al., 2009; Gulick et al., 2010; Conin et al., 2012), subduction of a seamount below the NE edge of the basin (Kimura et al., 2011), and changes in subduction accretion/erosion along the margin (e.g., Takano et al., 2013).

Detrital sediments deposited in the basin could have originated in distinct geological parts of the margin. The Nankai forearc is bordered by a <2000 m tall, NE-SW striking mountain range that includes a quiescent segment of the Honshu volcanic arc. The range broadly follows the orientation of the Median Tectonic Line (MTL), a major, tectonically active fault separating two contrasting geological domains in Honshu (Ito et al., 2009). The area NW of the MTL, or Inner Zone, is composed of a Jurassic accretionary complex (Mino-Tanba Belt) and Cretaceous low-P/T metamorphic rocks and associated granitic intrusives (Ryoke Belt). The area SE of the MTL, or Outer Zone, includes a Mesozoic to Miocene accretionary prism and its metamorphic equivalents (Sanbagawa and Shimanto Metamorphic Belts), with minor Neogene igneous rocks (Taira, 2001; Aoki et al., 2011; Geological Survey of Japan, 2012) (Fig. 1). The mountain range along Honshu shelf is interrupted north of the Kumano Basin by the Ise Bay, where the continental shelf extends locally ~65 km into the Inner and Outer Zones. In the NE, the Honshu volcanic arc has been colliding with the Izu-Bonin volcanic arc for the past 15 m.y. in the Izu Collision Zone (Amano, 1991). This collision has resulted in significant uplift and erosion of the Honshu and Izu volcanic arcs (Kimura et al., 2008; Okuzawa and Hisada, 2008).

Recent erosional products from the Collision Zone are transported downslope by turbidity currents through the Suruga Canyon and along the Nankai Trough, where they eventually accumulate and contribute to construction of the accretionary prism (Taira and Niitsuma, 1985; Soh and Tokuyama, 2002; Kimura et al. 2008) (Fig. 1). Similarly, igneous, metamorphic and sedimentary fragments reworked from the Inner and Outer Zones have been significant components of turbidites in the lower forearc (i.e., trench slope, trench-slope basins and trench) since the Miocene (De Rosa et al., 1986; Marsaglia et al., 1992; Fergusson, 2003; Underwood et al,. 2003; Underwood and Fergusson, 2005; Underwood and Moore, 2012; Clift et al., 2013; Usman et al., 2014). However, to date, constraints on the provenance of turbidites have been restricted to the modal composition of sandstones (e.g., Fergusson, 2003; Usman et al., 2014) and one zircon study (Clift et al., 2013). Although there is evidence that the morphology of the trench slope controlled distribution of turbidites during the Neogene (e.g., Underwood et al., 2003), patterns of detrital sedimentation associated with formation of the forearc basin remain to be determined.

3. Methods

Documenting temporal changes in the sources of detrital sediments deposited in the Kumano Basin and characterising possible effects of the basin development on lateral deflection of turbidity currents in the upper forearc were achieved using: (1) refined stratigraphic correlation of intra-basin drilling sites based on reflection seismic, logging, lithological and age data from the IODP; and (2), sediment provenance analysis based on compositional variations of detrital pyroxenes from a selection of river samples in Japan and IODP samples from the Kumano Basin and nearby slope environment.

This study includes the use of the first IODP drill cuttings, which were collected in the Kumano Basin at site C0009 during Expedition 319 (Saffer et al., 2010). The stratigraphic accuracy of these samples is discussed in detail in Appendix A (Supplementary File 1). In summary, these samples allow characterisation of major lithological changes downhole with great accuracy, including recognition of thin (<5 m thick) intervals of contrasting lithology (e.g., ash-rich interval interbedded with sandy

Corrected, unformatted version – full edited paper at http://doi.org/10.1016/j.epsl.2014.12.046

turbidites). Very limited mixing of detrital grains during retrieval of cuttings samples at site C0009 is of no consequence for the accuracy of our provenance analysis during different stages of evolution of the Kumano Basin.

3.1. Stratigraphic correlation

Three IODP drill sites were considered: (1) site C0009 in the central part of the Kumano Basin; (2) site C0002 in the outer part of the Kumano Basin; and (3), site C0001 in a trench-slope/piggyback basin ~5 km SW of the Kumano Basin (Fig. 1). Correlation of drill sites in the basin was achieved based on a seismic profile through sites C0009 and C0002 and IODP data (Fig. 2). We identified four regional unconformities or sequence boundaries (SB1 to SB4, from oldest to youngest) on the basis of erosional truncations, onlap and/or downlap surfaces (Fig. 2). The seismic units bounded by these unconformities are sequences that represent deposition during tectonically controlled phases of basin development. The seismic units are referred to as Unit 1 or Subunit 1A and Subunit 1B, Unit 2, and Unit 3 (Fig. 2). Fig. 4 shows flattened seismic sections on key unconformity surfaces to constrain better the basin formation at specific times. IHS Kingdom Suite software was used for seismic data interpretation and flattening of horizons. Logging data and lithostratigraphic descriptions of cores and drill cuttings were collected during IODP Expedition 314 and 319 (Kinoshita et al., 2008; Saffer et al., 2010). Among logging data, gamma ray and photoelectric factor (PEF) gave the best constraints on lithostratigraphic variations in the Kumano Basin (Fig. 3).

Depositional ages at drill sites C0001, C0002 and C0009 are based on nannoplankton ages collected during IODP Expeditions 315 and 319 (Kinoshita et al., 2008; Saffer et al., 2010) and post-cruise research by Kameo and Jiang (2013). Sedimentation rates at sites C0002 and C0009 are based on the interpretation given in Fig. S1. In the absence of sampling and determination of depositional ages for most of IODP Units I and II at site C0009, the sedimentation rate was assumed to be constant throughout this interval.

3.2. Sediment provenance analysis

Sediment provenance studies along the Nankai margin have been essentially constrained based on the framework grain composition of sandy sediments (i.e., quartz, feldspars and lithic fragments) using a Gazzi-Dickinson point counting technique (e.g., Ferguson, 2003; Usman et al., 2014). Although this approach can give valuable insight into source effects controlling the composition of detrital sediments (e.g., Dickinson and Suczek, 1979; Marsaglia and Ingersoll, 1992), hydrodynamic sorting during transport and deposition, and preferential preservation of some mineral species during transport and diagenesis are equally significant in controlling sediment composition (Morton and Hallsworth, 1999; Garzanti et al., 2009). As a result, interpretation of sediment provenance based on the modal abundance of framework grains (or heavy minerals) is often ambiguous. In contrast, approaches using single grain geochemical analysis or single grain geochronology are not affected by alteration, hydrodynamic and diagenetic effects and, thus, allow a more robust and detailed characterisation of provenance (von Eynatten and Dunkl, 2012). In the Nankai margin, geochronology of detrital zircons can be used to determine the relative contribution of the Inner, Outer and Collision Zones in turbidites (Clift et al., 2013). This approach notably allowed assessment of clastic flux to the Nankai Trough in SW Japan over the past 14 m.y. However, except for identification of material eroded from the Collision Zone, age patterns in Honshu do not have the level of spatial contrast required to outline lateral transport of sediments in the upper forearc.

To determine the provenance of sediment and assess longitudinal transport of turbidity currents in the forearc slope we use here detrital clinopyroxenes and orthopyroxenes as source tracers. The

composition of magmatic clinopyroxenes determined by microprobe analysis has a demonstrated value to determine provenance of sediments in volcanic environments (e.g., Nisbet and Pearce, 1977; Leterrier et al., 1982). We complement this approach by LA-ICP-MS analysis of Rare Earth Elements (REE), which allowed improved characterisation of sediment sources. In addition, we introduce the use of orthopyroxenes, which have not previously received much attention in provenance studies (von Eynatten and Dunkl, 2012), but that we show beneficially complement the analysis of clinopyroxenes.

29 samples of sand and poorly consolidated sandstones were collected at the mouth of 8 major rivers between the Kii Peninsula and the Izu Collision Zone (Figs 1 and S2) and at drill sites C0001, C0002 and C0009 (Table T1). Heavy minerals >64 µm were separated in a solution of Na-polytungstate. 1188 pyroxene grains ranging in size between ~100 and ~500 µm were handpicked under a microscope from heavy mineral separates, mounted in epoxy resin and polished for electron microprobe and LA-ICP-MS analysis. Analytical conditions are detailed in Appendix B (Supplementary File 2) and results with standard measurements are given in Tables T2-T4. All the clinopyroxenes used in this study are in the augite and diopside fields (Fig. S3). They generally have MgO >14 wt%, indicating that they crystallized in poorly fractionated, mafic to intermediate liquids. Consistency of the microprobe and LA-ICP-MS analyses is attested by the reproducibility of Ti measured by both techniques (Fig. S4).

4. Results

4.1. Tectono-stratigraphic subdivision of the Kumano Basin

Three main tectono-stratigraphic units are defined in the Kumano Basin based on recognition of major sequence boundaries (SB1-4, Fig. 2) combined with logging data, lithological observations and depositional ages collected by IODP expeditions at sites C0009 and C0002 (Konishita et al., 2009; Saffer et al., 2010) (Fig. 3). Tectono-stratigraphic Unit 1 between SB1 and SB3 consists of an interval of slow sedimentation (35-270 m/Ma) in a slope environment on top of the Nankai accretionary prism. SB1 is an erosional unconformity that marks a regional hiatus ~5.6 to 3.8 Ma on top of the prism (Moore et al. 2009; Underwood and Moore, 2012; Kameo and Jiang, 2013), whereas SB3 is a time transgressive surface marking the transition from slope sedimentation (Unit 1) to incipient basin infill (Unit 2). Unit 1 corresponds to IODP Units IIIA and IIIB at site C0009 (3.8 to 0.9 Ma) and IODP Unit III at site C0002 (3.8 to 1.6 Ma), which are composed of hemipelagic mud with few, thin beds of fine sand turbidites and ash deposits (Fig. 3). SB2 marks the contact between IODP units IIIA and IIIB at site C0009 and laps down on the accretionary prism NW of site C0002 (Figs 2-4). This boundary separates two distinct sedimentation regimes during deposition of Unit 1 that are included thereafter in tectono-sedimentary Subunits 1a and 1b (Fig. 2). Subunit 1a corresponds to small perched basin(s) documented by angular relations of sediments (Figs 2, 4) and a distinctive, high content in plant debris at site C0009 (Saffer et al., 2010). Subunit 1b is characterised by more transparent seismic reflectors compared to those of Subunit 1a (Fig. 2). It is also characterised by a mud-rich condensed interval at site C0002 (Kinoshita et al., 2009; Underwood and Moore, 2012) and a newly recognised condensed interval at site C0009 that correlates to low PEF values (Figs S1, 3).

Tectono-stratigraphic Unit 2 between SB3 and SB4 represents the first stage of infill of the Kumano Basin. SB4 is another time transgressive surface that corresponds to a major change in the direction of sediment onlaps from predominantly landward dipping reflectors (Unit 2) to seaward dipping reflectors (Unit 3) (Fig. 4). Sediments in Unit 2 occur in a stratigraphic interval including parts of IODP Unit II at site C0009 (0.9 to ~0.7 Ma) and IODP Units I and II at site C0002 (1.6 to ~0.3 Ma) (Fig. 3). The transition from Unit 1 to Unit 2 was accompanied by an abrupt increase in sedimentation rate to ~1067 m/Ma, which is linked to an increased supply of coarser-grained turbidites progressively

Corrected, unformatted version – full edited paper at http://doi.org/10.1016/j.epsl.2014.12.046

lapping on previous slope sediments towards the NW (Figs 2-4). Near the top of site C0002, close to IODP Units I-II boundary (~1.0-0.9 Ma), sedimentation rates decrease to ~108 m/Ma (Fig. 2, S1), which we consider reflect limited turbidite emplacement in the outer basin shortly before deposition of Unit 3. This is consistent with tilting of the basin and migration of the main depocenter towards the NW between 1.3 and 1.0 Ma as constrained by 3D seismic data (Gulick et al., 2010). However, our stratigraphic analysis and new age data from Site C0009 indicate that the transition from Unit 2 to Unit 3 was gradational and that it is not until SB4 (clearly <0.9 Ma at site C0009, Fig. S1) that a new regime of sedimentation had developed with persistent lapping of turbidites on the forearc high in the outer basin. Documenting details of this transition is beyond the scope of this study, but we note that basin tilting was accompanied by deformation of an intrabasinal high near site C0009 (Fig. 2), which partly controlled relocation of the depocenter in the central part of the basin shortly before deposition of Unit 3 (~1 Ma).

Tectono-stratigraphic Unit 3 includes all sequences above SB4, which were deposited after the main tilting phase of the Kumano Basin ~1.3-1.0 Ma (Gulick et al., 2010). This Unit corresponds to IODP Unit I and parts of IODP Unit II at site C0009 (~0.7 Ma and younger), and parts of IODP Unit I at site C0002 (~0.3 Ma old and younger) (Fig. 3). They consist of turbidite sequences with increased coarse sand toward the top of the basin. Seven mud-sand cycles occur in the upper part of IODP Unit I at site C0009, which are documented by gamma ray data (Fig. 3) and have an average recurrence of ~40 k.y. (7 cycles in 85-330 meters below sea floor [mbsf] interval with a constant sedimentation rate of ~865 m/Ma, Fig. 3).

4.2. Composition of pyroxenes in modern river sediments

Major and trace element contents of detrital pyroxenes found in modern river sediments outline compositionally distinct sources along the Japanese forearc, with significant differences between the Inner, Outer and Collision Zones. Detrital clinopyroxenes drained from the Outer Zone (i.e., found in the Kino, Kumano, Tenryu and Abe rivers, Figs 1 and S2) include both alkaline, MORB-like and calcalkaline arc affinities in Leterrier et al. (1982) discrimination diagrams (Fig. 5). A possible exception to this observation is the lack of clinopyroxenes with alkaline affinity in the Kumano river. In contrast, clinopyroxenes from the Inner Zone (i.e., found in the Kiso and Nagara rivers) essentially have a calcalkaline arc affinity. Clinopyroxenes from the Collision Zone (i.e., found in the Fuji and Kano rivers) have both calkalcaline arc and tholeiitic arc affinities. A broad Outer Zone source can therefore be defined based on the distinctive occurrence of clinopyroxenes with either alkaline or MORB-like affinities in the Kino, Kumano, Tenryu and Abe rivers. The origin of these pyroxenes is most likely associated with erosion of accreted oceanic crust (ocean floor and seamounts) exposed in Mesozoic-Cenozoic accretionary complexes. Similarly, the composition of clinopyroxenes in the Collision Zone is consistent with erosion of calcalkaline and tholeiitic volcanoes of the Izu-Bonin arc, whereas calcalkaline affinities observed in samples from the Inner Zone likely represent erosion of older arc volcanoes formed on the Japanese continental crust (Fig. S2).

REE contents of detrital clinopyroxenes display a large variability among source areas, which can be used to unravel parts of the compositional overlaps displayed in Leterrier et al. (1982) diagrams. Two additional detrital sources are defined using a La/Sm versus Dy/Yb diagram (Fig. 6): (1) a broad Inner Zone source with distinctive, high La/Sm and low Dy/Yb clinopyroxenes; and (2), an Abe river source with characteristic, high Dy/Yb and medium to low La/Sm clinopyroxenes.

Finally, three compositionally distinct detrital sources (of unclear origins) are outlined by orthopyroxenes in the Kumano, Tenryu and Kano rivers using % ferrosilite versus Al, % ferrosilite versus Na and % ferrosilite versus Ca diagrams (Fig. 7). This is an important result showing that orthopyroxenes can be used to identify specific sediment sources. In summary, the compositional

variability of the pyroxenes in our river samples defines seven sediment sources: (1) a broad Outer Zone source; (2) a Kiso and Nagara rivers (Inner Zone) source; (3) a Fuji and Kano rivers (Collision Zone) source; (4) a Kumano river source; (5) a Tenryu river source; (6) an Abe river source; and (7), a Kano river source.

4.3. Composition and provenance of detrital pyroxenes at drill sites

The provenance of sandy sediments at IODP sites C0009, C0002 and C0001 is constrained based on comparison of the composition of detrital pyroxenes from core samples and drill cuttings with that of pyroxenes from river sediments. This approach assumes limited compositional variation of source areas and no significant changes in on-land erosional and transport processes in the past 2.5 Ma. This assumption is in good agreement with broadly constant exhumation rates across the studied area and magmatic quiescence in SW Honshu during this period (Kimura et al., 2005; 2008; Clift et al., 2013).

Downhole decrease of pyroxene content and frequent etching of amphibole and pyroxene grains were observed at sites C0002 and C0009 in the Kumano Basin, which is indicative of instability of mineral phases during diagenesis (Velbel, 2007). However, pyroxenes occur down to 968 mbsf at site C0009 (Table T1), which is ~400 m below the commonly accepted depth of stability of amphiboles and pyroxenes (e.g., Morton and Hallworth, 2007). Good preservation of pyroxenes in the Kumano Basin may be related to the relatively young age of the sediments, high sedimentation rates and poor consolidation of formations that together suggest limited diagenesis. The preservation of these minerals may be also related to low geothermal gradients in forearc environments relative to other tectonic settings. Because dissolution during diagenesis lowered the number of pyroxenes available in our deepest samples, the pyroxenes were considered collectively in each tectono-stratigraphic unit. This approach, combined with the large compositional spectrum of pyroxenes and characterisation of their variability in several compositional spaces, allows robust determination of sediment sources.

Clinopyroxenes at site C0009 have a consistent compositional range throughout development of the basin (Units 1 to 3), with an assemblage of alkaline, MORB-like and calcalkaline arc affinities in Leterrier et al. (1982) diagrams (Fig. 5). The alkaline and MORB-like affinities unambiguously indicate a sediment contribution from the Outer Zone. An absence of contribution from the Collision Zone is documented by a lack of tholeiitic arc signature. In addition, REE contents of clinopyroxenes show that sand/sandstone sampled at site C0009 did not source in Abe river and partly originate from the Inner Zone (Fig. 6). The compositions of orthopyroxenes at site C0009 are consistent with other observations, further outlining a clear Kumano source, without evidence for contribution from Tenryu and Abe rivers (Fig. 7). Growing influence of material supplied by the Kumano river during infill of the Kumano Basin is supported by an increased fraction of orthopyroxenes delivered by the Kumano river from Unit 1 (7% of 27 grains with % ferrosilite > 49) to Unit 2 (13% of 69 grains with % ferrosilite > 49) and Unit 3 (36% of 50 grains with % ferrosilite > 49).

The composition of pyroxenes in Unit 2 at site C0002 (~1.1 to ~0.3 Ma) of the Kumano Basin outlines a predominant contribution from the Inner Zone, with clinopyroxenes with calcalkaline arc affinities in Leterrier et al. (1982) diagrams (Fig. 5) and REE contents characteristic of Nagara and Kiso rivers (Fig. 6). Orthopyroxenes at site C0002 show some compositional overlap with those at site C0009, with evidence for a minor contribution from a Kumano source and a larger influence from an unknown source with high Al values (Fig. 6). No influence from the Collision Zone or Tenryu and Abe rivers is recorded.

Detrital pyroxenes sampled out of the Kumano Basin at site C0001 have a large compositional range supporting Outer and Inner Zones origins (Figs 5-7). Clinopyroxenes have alkaline, MORB-like and calcalkaline arc affinities in Leterrier et al. (1982) diagrams (Fig. 5). Alkaline affinities characteristic of an Outer Zone source are, however, restricted to sample 184-3, even though all our samples at site C0001 are included in a 5.4 m thick turbidite interval deposited broadly synchronously ~2.2 Ma. Sediment sources at site C0001 are partly distinct from those at sites C0009 and C0002 in the past 2.5 m.y., with the occurrence of few clinopyroxenes with tholeiitic arc affinities in Leterrier et al. (1982) diagrams (Fig. 5) and abundant clinopyroxenes with La/Sm<0.3 (Fig. 6). This documents an Izu-Bonin arc source with a compositional range, albeit slightly distinct from that of pyroxene assemblages found in recent Fuji and Kano rivers. In addition, site C0001 lacks Kumano-derived orthopyroxenes observed at sites C0009 and C0002 (Fig. 7). These observations indicate that turbidites at site C0001 were transported from compositionally distinct sources during the early Quaternary, including the Inner Zone, Outer Zone and the Izu-Bonin arc, but excluding Kumano and Tenryu sources.

5. Discussion

Sediment routing during development of the Kumano Basin is discussed below in a model of Quaternary evolution of the upper forearc based on integration of our results and existing structural and sedimentological constraints at a regional scale (Fig. 8).

5.1. Initiation of the Kumano Basin

The initiation of the Kumano Basin created a large accommodation space in the upper forearc, which is expected to have strongly modified sediment routing along the margin (e.g., Underwood & Moore, 2012; Takano et al., 2013; Usman et al., 2014). Determining the time of basin initiation, therefore, is critical in reconstructing sedimentation patterns in the forearc region. The initiation of the Kumano Basin has previously been associated with onset of fast sedimentation at site C0002 ~1.6 Ma (Kinoshita et al., 2009; Strasser et al., 2009). Because this age predates that of activation of the megasplay fault by ~0.4 m.yr., it has been assumed in recent studies that basin initiation had no causal relationship with fault activity (e.g., Strasser et al., 2009). However, our tectono-stratigraphic analysis indicates that onset of fast sedimentation at site C0002 corresponds to time transgressive boundary SB3 between Units 1 and 2, and that basin sediments of Unit 2 first deposited farther SE before prograding towards the NW and overlapping slope sediments of Unit 1 at site C0002 (Figs 3, 4). These observations indicate that onset of fast sedimentation at site C0002 only represents a minimal age of basin formation. A better age estimate of the initiation can be obtained by calculating time elapsed between the first record of deposition of Unit 2 in the basin and its onlap at site C0002 ~1.6 Ma. This approach yields a ~1.93 Ma age of basin initiation (using a thickness of ~430 m for the interval of basin sediments stratigraphically below site C0002 and a constant sedimentation rate of 1067 m/Ma within this interval). This age broadly corresponds to that of initiation of the megasplay fault ~1.97 Ma as an out-of-sequence frontal thrust (Strasser et al., 2009, 2011; Kimura et al., 2011). Therefore, we follow here the model by Moore et al. (2007) in which the initiation of the Kumano Basin is caused by formation of the megasplay fault during a phase of rapid growth of the prism (Fig. 8). We discuss below changes in sedimentation routing associated with this event and the maturation of the Kumano Basin.

5.2. Transition from trench slope to forearc basin sedimentation

Sedimentation in the Kumano Basin was preceded by deposition of Unit 1 in a slope environment, with a change ~2.8 Ma from small perched basins (Subunit 1a) to draping deposits (Subunit 1b). We propose that this change was primarily controlled by frontal accretion in the prism and transition of sites C0009 and C0002 from a frontal thrust zone to an inner prism setting (Fig. 8). This interpretation is well supported by sediment accretion in the earliest Quaternary at sites C0001, C0004, and C0008 (Kinoshota et al., 2009; Strasser et al., 2009), possibly coeval changes in the structural regime in the margin basement at site C0009 (Hayman et al., 2012), and our provenance results (see below). In addition, spatially restricted basins such as those in Subunit 1a ~3.8 to 2.8 Ma and at site C0001 ~2.2 Ma are typical features in the frontal thrust zone of accretionary prisms (e.g., Moore and Karig, 1976; Kawamura et al., 2009).

Sediments deposited before ~2.8 Ma at site C0009 (Subunit 1a) contain abundant plant fragments not documented in other nearby IODP sites (Kinoshita et al., 2009; Saffer et al., 2010; Strasser et al., 2014). Although no pyroxene could be recovered in Subunit 1a, these plant fragments attest for a terrestrial supply from Honshu down to the outer margin. Deposition in small perched basins indicates that turbidity currents flowing downslope were deflected and funnelled along trench-slope basin(s), in a way similar to that observed today along the outer Nankai Margin (Underwood et al., 2003). The condensed interval in IODP Unit III at site C0002 (~3.8 to 1.6 Ma) was deposited in an environment sheltered from turbidity currents. This site was a topographic high probably created by deformation of the accretionary prism in the early Quaternary (Fig. 4), which persisted until burial under infill deposits in the Kumano Basin ~1.6 Ma.

Detrital pyroxenes deposited in slope sediments at site C0009 from 2.8 to 0.9 Ma indicate that turbidity currents were carrying material sourced in the Inner and Outer Zones down to the outer forearc. Transport of materials from these zones down to the trench is consistent with previous provenance studies at a regional scale (e.g., Fergusson, 2003; Clift et al., 2013) and earlier deposition of plant fragments at this site (Saffer et al., 2010). Importantly, pyroxene data further indicate that longitudinal currents proceeding from, e.g., the Tenryu river or Collizion Zone, did not exist at Site C0009 before development of the Kumano Basin. This is in good agreement with the occurrence of only elongated, NW-SE striking fans in the slope at this time (Takano et al., 2013). The absence of longitudinal transport along the forearc slope was probably related to smooth topography above site C0002, with several transverse canyons allowing sediment delivery from Honshu down to the trench (Fig. 8). This environment contrasts with that at site C0001 (~2.2 Ma), where pyroxenes record a clear input from the Izu-Bonin volcanic arc in addition to the Inner and Outer Zones. Volcanic fragments found in the modern Nankai Trough clearly indicate a detrital input from the Collision Zone through the Suruga Canyon (De Rosa et al., 1986). The existence of a similar process earlier during evolution of the margin has been suggested based on the framework grain composition of sand/sandstone (e.g., Fergusson, 2003; Underwood and Fergusson, 2005; Usman et al., 2014) but could not be confirmed by recent analysis of detrital zircons (Clift et al., 2013). Pyroxenes from site C0001 are therefore the first unequivocal evidence for long-distance axial transport from the Collision Zone along the Nankai Trough in the early Quaternary. They additionally provide strong support for location of site C0001 in close proximity to the trench ~0.3 m.y. before initiation of the Kumano Basin (Fig. 8).

5.3. Sediment routing during development of the Kumano Basin

The confinement of density currents is a significant mechanism in forearc and foreland basins, where longitudinal deflection of turbidity currents occurs until nearly complete infill of accommodation space or formation of canyons incising the outer ridge of the basin (e.g., Dickinson and Seeley, 1979; Sinclair and Tomasso, 2002). Along the Nankai forearc, initiation of the megasplay fault in the early Quaternary and associated development of a forearc high in the outer margin resulted in onset of

Corrected, unformatted version – full edited paper at http://doi.org/10.1016/j.epsl.2014.12.046

the Kumano Basin and development of a large accommodation space (Fig. 8). Turbidite confinement during the first phase of basin development is well documented by a remarkable increase in local sedimentation rates from <300 m/Ma to >800 m/Ma (Fig. 3), which is associated with deposition of Unit 2 progressively lapping towards the NW on Unit 3 until major basin tilting in the middle Quaternary (Gulick et al., 2010; this study). Detrital pyroxenes document however that longitudinal transport of material was very limited, with a proximal Outer Zone source (e.g., the Kumano river), without evidence for transport from distant rivers along the Outer Zone (i.e., Tenryu and Abe rivers) or the Collision Zone. Limited longitudinal transport into the basin was probably related to persistent canyons incising the upper slope. Pyroxene data further document an Inner Zone source that supports supply of material to the early Kumano Basin through the Ise Bay (Fig. 8). Metamorphic material sourced in the Outer Zone is preserved in ~1.67 to 1.05 Ma old turbidites at site C0018, which deposited SW of the Kumano Basin in a trench-slope basin (Usman et al., 2014). This suggests frequent spilling of material over the margin of the Kumano Basin and very limited deflection of density currents before the tilting event (Fig. 8). Uplift of the basin margin likely remained low during this period due to limited activity of the megasplay fault (Gulick et al., 2010; Kimura et al., 2011; Strasser et al., 2011).

Major tilting of the basin between 1.3 and 1.0 Ma resulted in migration of the main depocenter towards the NW (Gulick et al., 2010) with diachronous deposition of Unit 3 over Unit 2. Several observations indicate this tilting led to a new basin configuration with development of a prominent ridge in the outer basin and increased turbidite confinement (Fig. 8). First, the tilting event was associated with significant decrease of the sedimentation rate from 1067 to 108 m/Ma in the outer basin at site C0002, whereas sedimentation rate remained high in the inner basin (>800 m/Ma) at site C0009. Second, tilting of the Kumano Basin was accompanied in the trench-slope basin at site C0018 by persistent reduction in abundance of metamorphic grains from the Inner and Outer Zone relative to volcanic grains from, possibly, the Collision Zone, which could reflect changes in flux of material from different sources (Usman et al., 2014). Finally, detrital orthopyroxenes in the inner basin at site C0009 show increased supply from the Kumano river from Units 1 to 3, which is consistent with improved confinement of material from proximal sources through time. However, similarly to sedimentation prior to basin tilting, detrital pyroxenes clearly show that longitudinal transport of material from the NE was limited, without contribution from the Tenryu river or Collision Zone. As proposed above we speculate that transverse canyons have been a major limiting factor of longitudinal transport in the upper forearc. Subduction of a seamount since ~1 Ma (Kimura et al., 2011) has resulted in severe disruption along the NE margin of the Kumano Basin (Fig. 1). Subduction of topographic features even of small size can promote development of large canyons (Soh and Tokuyama, 2002) and, thus, it is very likely that canyon development in response to seamount subduction has played a recurrent role in controlling sediment routing along the Nankai accretionary prism during the Quaternary.

Detrital pyroxenes show clastic flux from the Inner Zone persisted in the Kumano Basin after the tilting event. Material most likely transited across the MTL down to the basin through the Ise Bay and Anoriguchi Canyon (Figs 1, 8). Sedimentological variations in the NE part of the Kumano Basin close to the Anoriguchi Canyon indicate that the terrigenous flux was affected by eustatic changes at least during the last glacial cycle (Omura and Ikehara, 2010). A delta system has been active in the recent Quaternary in the Ise Bay (Masuda and Iwabuchi 2003; Saegusa et al., 2011) and Omura and Ikehara (2010) proposed that sedimentation changes in the NE Kumano Basin since the last deglaciation was due to variations in accommodation space in the Ise Bay, with more terrigenous material carried downslope during lowstand and increased deposition of this material in the bay during highstand. Similarly, we propose that ~40 k.y.-long mud-sand cycles documented by gamma ray data at site C0009 reflect Milankovitch cycles and climate forcing on turbidite sedimentation during the past ~0.3 m.y. This suggests that stronger currents or tectonics prevailed during earlier basin evolution or that migration of the depocenter close to the shore was required before eustatic

effects could be expressed in the sedimentary record. In both cases, sediments accumulated for ~1.8 m.y. in the basin before a clear climatic signal was expressed and, thus, basin maturation was likely key to development of this signal.

6. Conclusions

This study shows that an integrated analysis of stratigraphy and pyroxene provenance offers valuable insight into the evolution of sedimentation patterns in the upper forearc environment, in particular during development of a large basin with diachronous units. Use of REE contents in clinopyroxenes and the composition of orthopyroxenes together with existing discrimination diagrams (e.g., Leterrier et al., 1982) is a powerful approach to characterise sediment flow routing in volcanic environments. In addition, this study demonstrates that drill cuttings can make a valid substitute to core samples in provenance studies.

Our results show that sedimentation in the Kumano Basin records different stages of development from trench-slope to upper-forearc environments during development of the Nankai accretionary prism. The transition was accompanied by readjustment of sediment flow routing to geometrical changes of the slope. In the early Quaternary, shortly prior to basin initiation, long-distance axial transport from the Izu-Bonin arc was coeval with transport downslope from distant Inner Zone sources and proximal Outer Zone sources. This sedimentation pattern was replaced in the early Kumano Basin by predominantly transverse transport of material from the Inner Zone and proximal Outer Zone, with frequent spilling over the basin edge into the trench slope environment. Turbidite confinement increased in the basin after a major tilting event in the middle Quaternary, but sediment flow routing remained mostly unchanged, with only limited longitudinal transport from the Ise Bay. In the late Quaternary, climate cycles are clearly expressed in turbidite sequences of the basin due to eustatic variations and changes in flux of terrigenous material transiting/deposited along the shelf. The lack of long-distance longitudinal flows in the upper forearc during development of the Kumano Basin suggests that canyons (possibly triggered by subducting seamounts) greatly facilitated transverse transport of material downslope from the upper forearc. This is a significant contrast with sediment flow routing in the trench slope environment and foreland basins.

ACKNOWLEDGEMENT

This research used samples collected by D.M.B. and H.M. on-board D/V Chikyu during NanTroSEIZE stages 1 and 2 of the Integrated Ocean Drilling Program (IODP). We are thankful to team members of Expedition 319, in particular Natalia Efimenko, Kuniyo Kawabata, Anja Schleicher, and the expedition co-chiefs for stimulating discussions on the use of the first drill cuttings of the IODP. Maxim Portnyagin provided generous help during preparation and analysis of the pyroxenes. We thank Ulrike Westernströer (University of Kiel) and Mario Thoener (GEOMAR) for their help during LA-ICP-MS and microprobe analyses. Lesley Cherns kindly accepted to polish the style of the English before final submission. Raymond Ingersoll and An Yin (Editor) are thanked for their review that helped improve the quality of this paper. This research benefited from the support of the Swiss National Science Foundation to the IODP (D.M.B) and the “International Ocean Discovery Program" of the Ministry of Oceans and Fisheries, Korea (D.C.). It developed during the tenure of postdoctoral fellowships (D.M.B.) at the Australian National University and GEOMAR (Swiss National Science Foundation grants #PBLA22-122660 and #PA00P2-134128/1).

REFERENCES

Amano, K., 1991. Multiple collision tectonics of the South Fossa Magna in central Japan. Modern Geology 15, 315-329.

Aoki, K., Maruyama, S., Isozaki, Y., Otoh, S.,Yanai, S., 2011, Recognition of the Shimanto HP metamorphic belt within the traditional Sanbagawa HP metamorphic belt: New perspectives of the Cretaceous - Paleogene tectonics in Japan. Journal of Asian Earth Sciences 42, 355 - 369.

Bangs, N.L.B., Moore, G.F., Gulick, S.P.S., Pangborn, E.M., Tobin, H.J., Kuramoto, S., Taira, A., 2009. Broad, weak regions of the Nankai Megathrust and implications for shallow coseismic slip. Earth and Planetary Science Letters 284, 44-49.

Clift, P.D., Carter, A., Nicholson, U., Masago, H., 2013. Zircon and apatite thermochronology of the Nankai Trough accretionary prism and trench, Japan: Sediment transport in an active and collisional margin setting. Tectonics 32, 377-395.

Conin, M., Henry, P., Godard, V., Bourlange, S., 2012. Splay fault slip in a subduction margin, a new model of evolution. Earth and Planetary Science Letters 341–344, 170-175.

De Rosa, R., Zuffa, G.G., Taira, A., Leggett, J.K., 1986. Petrography of trench sands from the Nankai Trough, southwest Japan: implications for long-distance turbidite transportation. Geological Magazine 123, 477-486.

Dickinson, W.R., Seely, D.R., 1979. Structure and Stratigraphy of Forearc Regions. AAPG Bulletin 63, 2-31.

Dickinson, W.R., Suczek, C.A., 1979. Plate tectonics and sandstone compositions. AAPG Bulletin 63, 2164-2182.

Dickinson, W.R., 1995. Forearc basins, in: Busby, C.J., Ingersoll, R.V. (Eds.) Tectonics of sedimentary basins: Cambridge, Blackwell, pp. 221-261.

Fergusson, C.L., 2003. Provenance of Miocene-Pleistocene turbidite sands and sandstones, Nankai Trough, Ocean Drilling Program Leg 190, in: Mikada, H., Moore, G.F., Taira, A., Becker, K., Moore, J.C., Klaus, A. (Eds.), Proceedings of the ODP, Scientific results, 190/196.

Fuller, C.W., Willett, S.D., Brandon, M.T., 2006. Formation of forearc basins and their influence on subduction zone earthquakes. Geology 34, 65-68.

Geological Survey of Japan, 2012. Seamless digital geological map of Japan 1: 200,000. Research Information Database DB084, Geological Survey of Japan, National Institute of Advanced Industrial Science and Technology.

Gulick, S.P.S., Bangs, N.L.B., Moore, G.F., Ashi, J., Martin, K.M., Sawyer, D.S., Tobin, H.J., Kuramoto, S.i., Taira, A., 2010. Rapid forearc basin uplift and megasplay fault development from 3D seismic images of Nankai Margin off Kii Peninsula, Japan. Earth and Planetary Science Letters 300, 55-62.

Hayman, N.W., Timothy B, B., Lisa C, M., Kyuichi, K., Toshiya, K., Cassandra M, B., Anja M, S., Gary J, H., 2012. Structural evolution of an inner accretionary wedge and forearc basin initiation, Nankai margin, Japan. Earth and Planetary Science Letters 353â€“354, 163-172.

Ito, T., Kojima, Y., Kodaira, S., Sato, H., Kaneda, Y., Iwasaki, T., Kurashimo, E., Tsumura, N., Fujiwara, A., Miyauchi, T., Hirata, N., Harder, S., Miller, K., Murata, A., Yamakita, S., Onishi, M., Abe, S., Sato, T.,

Ikawa, T., 2009. Crustal structure of southwest Japan, revealed by the integrated seismic experiment Southwest Japan 2002. Tectonophysics 472, 124-134.

Kameo, K., and Jiang, S., 2013. Data report: calcareous nannofossil biostratigraphy of Site C0009, Expedition 319. In Saffer, D., McNeill, L., Byrne, T., Araki, E., Toczko, S., Eguchi, N., Takahashi, K., and the Expedition 319 Scientists, Proc. IODP, 330: Tokyo (Integrated Ocean Drilling Program Management International, Inc.). doi:10.2204/iodp.proc.319.202.2013

Kimura, G., Kitamura, Y., Yamaguchi, A., Raimbourg, H., 2008. Links among mountain building, surface erosion, and growth of an accretionary prism in a subduction zone - An example from southwest Japan. Geological Society of America Special Papers 436, 391-403.

Kimura, G., Moore, G.F., Strasser, M., Screaton, E., Curewitz, D., Streiff, C., Tobin, H., 2011. Spatial and temporal evolution of the megasplay fault in the Nankai Trough. Geochemistry Geophysics Geosystems 12, Q0A008.

Kimura, J.-I., Stern, R.J., Yoshida, T., 2005. Reinitiation of subduction and magmatic responses in SW Japan during Neogene time. Geological Society of America Bulletin 117, 969-986.

Kinoshita, M., Tobin, H., Ashi, J., Kimura, G., Lallemant, S., Screaton, E.J., Curewitz, D., Masago, H., Moe, K.T., and the Expedition 314/315/316 Scientists, 2009. Proc. IODP, 314/315/316: Washington, DC (Integrated Ocean Drilling Program Management International, Inc.). doi:10.2204/ iodp.proc.314315316.2009

Leterrier, J., Maury, R., Thonon, P., Girard, D., Marchal, M., 1982. Clinopyroxene composition as a method of identification of the magmatic affinities of paleo-volcanic series. Earth and Planetary Science Letters 59, 139-154.

Marsaglia, K.M., Ingersoll, R.V., 1992. Compositional trends in arc-related, deep-marine sand and sandstone: a reassessment of magmatic-arc provenance. Geological Society of America Bulletin 104, 1637-1649.

Marsaglia, K.M., Ingersoll, R.V., Packer, B.M., 1992. Tectonic evolution of the Japanese islands as reflected in modal compositions of Cenozoic forearc and backarc sand and sandstone. Tectonics 11, 1028-1044.

Martin, K.M., Gulick, S.P.S., Bangs, N.L.B., Moore, G.F., Ashi, J., Park, J.-O., Kuramoto, S.i., Taira, A., 2010. Possible strain partitioning structure between the Kumano fore-arc basin and the slope of the Nankai Trough accretionary prism. Geochemistry, Geophysics, Geosystems 11, Q0AD02.

Masuda, F., Iwabuchi, Y., 2003. High-accuracy synchronism for seismic reflectors and 14C ages: Holocene prodelta succession of the Kiso River, central Japan. Marine Geology 199, 7-12.

Melnick, D., Echtler, H.P., 2006. Inversion of forearc basins in south-central Chile caused by rapid glacial age trench fill. Geology 34, 709-712.

Moore, G.F., Bangs, N.L., Taira, A., Kuramoto, S., Pangborn, E., Tobin, H.J., 2007. Three-Dimensional Splay Fault Geometry and Implications for Tsunami Generation. Science 318, 1128-1131.

Moore, G.F., Park, J.-O., Bangs, N.L., Gulick, S.P., Tobin, H.J., Nakamura, Y., Sato, S., Tsuji, T., Yoro, T., Tanaka, H., Uraki, S., Kido, Y., Sanada, Y., Kuramoto, S., and Taira, A., 2009. Structural and seismic stratigraphic framework of the NanTroSEIZE Stage 1 transect. In Kinoshita, M., Tobin, H., Ashi, J., Kimura, G., Lallemant, S., Screaton, E.J., Curewitz, D., Masago, H., Moe, K.T., and the Expedition 314/315/316 Scientists, Proc. IODP, 314/315/316: Washington, DC (Integrated Ocean Drilling Program Management International, Inc.). doi:10.2204/iodp.proc.314315316.102.2009

Morton, A.C., Hallsworth, C., 2007. Chapter 7 Stability of Detrital Heavy Minerals During Burial Diagenesis, in: Maria, A.M., David, T.W. (Eds.), Developments in Sedimentology. Elsevier, pp. 215-245.

Morton, A.C., Hallsworth, C.R., 1999. Processes controlling the composition of heavy mineral assemblages in sandstones. Sedimentary Geology 124, 3-29.

Nisbet, E.G., Pearce, J.A., 1977. Clinopyroxene composition in mafic lavas from different tectonic settings. Contributions to Mineralogy and Petrology 63, 149-160.

Okuzawa, K., Hisada, K.-i., 2008. Temporal changes in the composition of Miocene sandstone related to collision between the Honshu and Izu Arcs, central Japan. Geological Society of America Special Papers 436, 185-198.

Omura, A., Ikehara, K., 2010. Deep-sea sedimentation controlled by sea-level rise during the last deglaciation, an example from the Kumano Trough, Japan. Marine Geology 274, 177-186.

Saegusa, Y., Sugai, T., Ogami, T., Kashima, K., Sasao, E., 2011. Reconstruction of Holocene environmental changes in the Kiso-Ibi-Nagara compound river delta, Nobi Plain, central Japan, by diatom analyses of drilling cores. Quaternary International 230, 67-77.

Saffer, D., McNeill, L., Byrne, T., Araki, E., Toczko, S., Eguchi, N., Takahashi, K., and the Expedition 319 Scientists, 2010. Proc. IODP, 319: Tokyo (Integrated Ocean Drilling Program Management International, Inc.). doi:10.2204/iodp.proc.319.2010

Seno, T., Stein, S., Gripp, A.E., 1993. A model for the motion of the Philippine Sea Plate consistent with NUVEL-1 and geological data. Journal of Geophysical Research: Solid Earth 98, 17941-17948.

Simpson, G.D.H., 2010. Formation of accretionary prisms influenced by sediment subduction and supplied by sediments from adjacent continents. Geology 38, 131-134.

Sinclair, H.D., Tomasso, M., 2002. Depositional Evolution of Confined Turbidite Basins. Journal of Sedimentary Research 72, 451-456.

Soh, W., Tokuyama, H., 2002. Rejuvenation of submarine canyon associated with ridge subduction, Tenryu Canyon, off Tokai, central Japan. Marine Geology 187, 203-220.

Strasser, M., Moore, G.F., Kimura, G., Kitamura, Y., Kopf, A.J., Lallemant, S., Park, J.O., Screaton, E.J., Su, X., Underwood, M.B., Zhao, X., 2009. Origin and evolution of a splay fault in the Nankai accretionary wedge. Nature Geoscience 2, 648-652.

Strasser, M., Dugan, B., Kanagawa, K., Moore, G.F., Toczko, S., Maeda, L., and the Expedition 338 Scientists, 2014. Proc. IODP, 338: Yokohama (Integrated Ocean Drilling Program). doi:10.2204/iodp.proc.338.2014

Taira, A., 2001. Tectonic Evolution of the Japanese Island Arc System. Annual Review of Earth and Planetary Sciences 29, 109-134.

Taira, A., Niitsuma, N., 1985. Turbiditic sedimentation in the Nankai Trough as interpreted from magnetic fabric, grain size, and detrital modal analyses. Initial Reports of the Deep Sea Drilling Project 87, 611-632.

Takano, O., Itoh, Y., Kusumoto, S., 2013. Variation in Forearc Basin Configuration and Basin-filling Depositional Systems as a Function of Trench Slope Break Development and Strike-Slip Movement: Examples from the Cenozoic Ishikari–Sanriku-Oki and Tokai-Oki–Kumano-Nada Forearc Basins,

Japan, in: Y., Itoh (Ed.), Mechanism of Sedimentary Basin Formation - Multidisciplinary Approach on Active Plate Margins, InTech, pp. 3-25.

Underwood, M.B., Fergusson, C.L., 2005. Late Cenozoic evolution of the Nankai trench-slope system: evidence from sand petrography and clay mineralogy, in: Hodgson, D.M., Flint, S.S. (Eds.), Geological Society, London, Special Publications, pp. 113-129.

Underwood, M.B., Karig, D.E., 1980. Role of submarine canyons in trench and trench-slope sedimentation. Geology 8, 432-436.

Underwood, M.B., Moore, G.F., 2012. Evolution of Sedimentary Environments in the Subduction Zone v of Southwest Japan: Recent Results from the NanTroSEIZE Kumano Transect, in: Busby, C., Azor, A. (Eds.), Tectonics of Sedimentary Basins: Recent Advances. John Wiley & Sons, Ltd, pp. 310-328.

Underwood, M.B., Moore, G.F., Taira, A., Klaus, A., Wilson, M.E.J., Fergusson, C.L., Hirano, S., Steurer, J., Party, t.L.S.S., 2003. Sedimentary and Tectonic Evolution of a Trench-Slope Basin in the Nankai Subduction Zone of Southwest Japan. Journal of Sedimentary Research 73, 589-602.

Usman, M., Masago, H., Winkler, W., Strasser, M., 2014. Mid-Quaternary decoupling of sediment routing in the Nankai Forearc revealed by provenance analysis of turbiditic sands. Int J Earth Sci (Geol Rundsch) 103, 1141-1161.

Velbel, M.A., 2007. Surface Textures and Dissolution Processes of Heavy Minerals in the Sedimentary Cycle: Examples from Pyroxenes and Amphiboles, in: Maria, A.M., David, T.W. (Eds.), Developments in Sedimentology. Elsevier, pp. 113-150.

von Eynatten, H., Dunkl, I., 2012. Assessing the sediment factory: The role of single grain analysis. Earth-Science Reviews 115, 97-120.

Wang, K., Hu, Y., von Huene, R., Kukowski, N., 2010. Interplate earthquakes as a driver of shallow subduction erosion. Geology 38, 431-434.

FIGURES

Figure 1. Tectonic and geologic setting of the Kumano Basin. Sampled localities include IODP sites C0002 and C0009 in the Kumano Basin, IODP site C0001 from a nearby trench-slope basin and 8 major rivers representative of sediment sources in the Inner Zone, Outer Zone and Collision Zone in Japan. Geology modified from Fergusson (2003). Bathymetry from GeoMapApp (data retrieved from http://www.geomapapp.org, 2012).

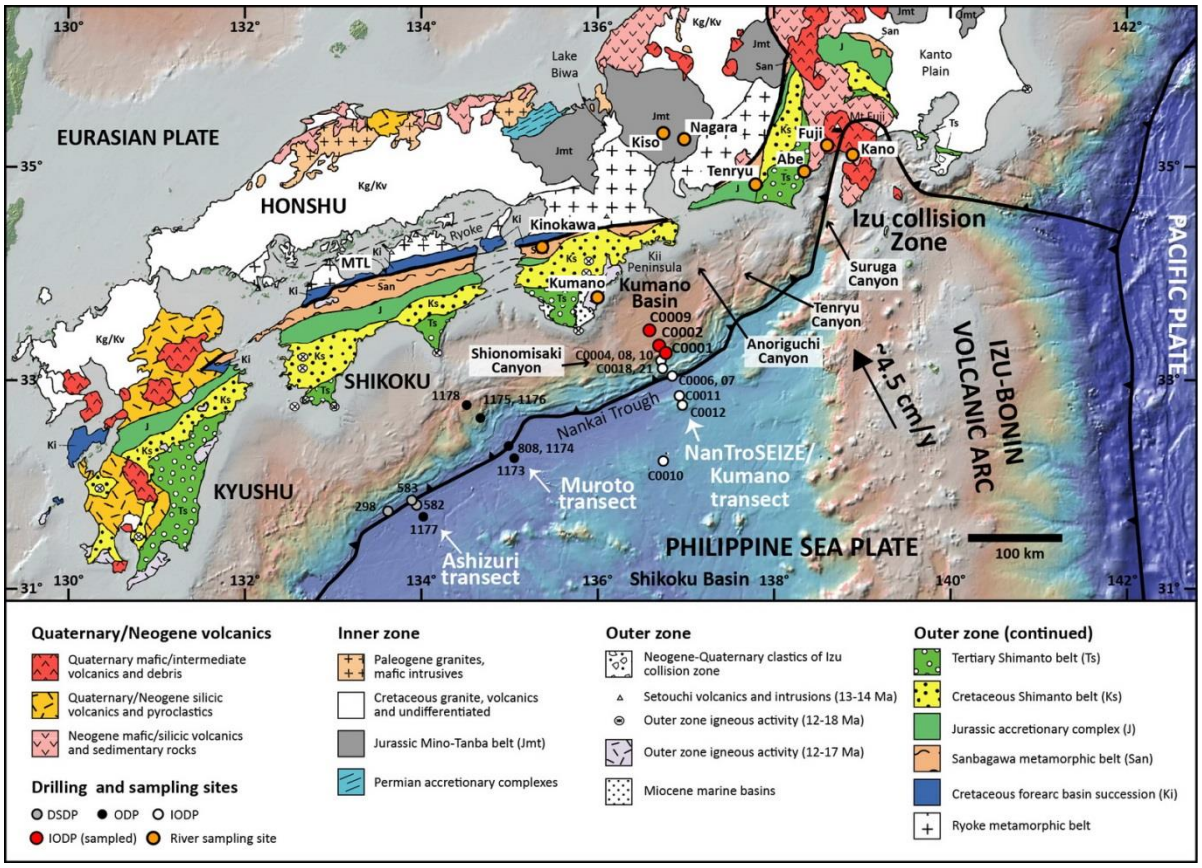

Corrected, unformatted version – full edited paper at http://doi.org/10.1016/j.epsl.2014.12.046

Figure 2. Seismic profile of the Kumano Basin. Inset (A) modified from Moore et al. (2009).

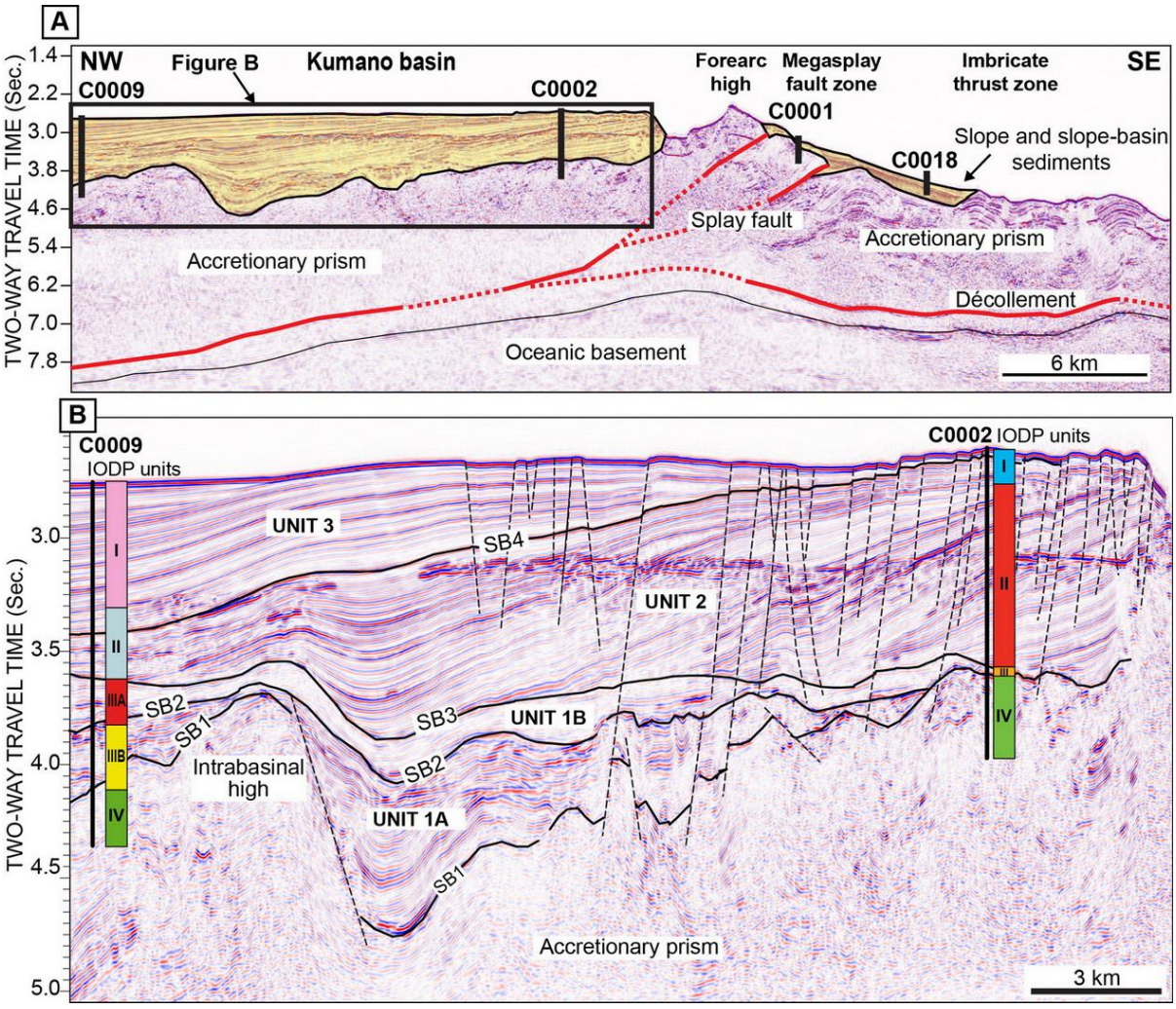

Corrected, unformatted version – full edited paper at http://doi.org/10.1016/j.epsl.2014.12.046

Figure 3. Stratigraphic correlation of drill sites C0002 and C0009 in the Kumano Basin, including IODP Units, newly-defined tectono-stratigraphic units and analysed samples. Lithological and logging data are from Kinoshita et al. (2008) and Saffer et al. (2010). Age data are from the same sources and Kameo and Jiang (2003). Sedimentation rates are based on new estimates as detailed under Section 3.1. and in Fig. S1.

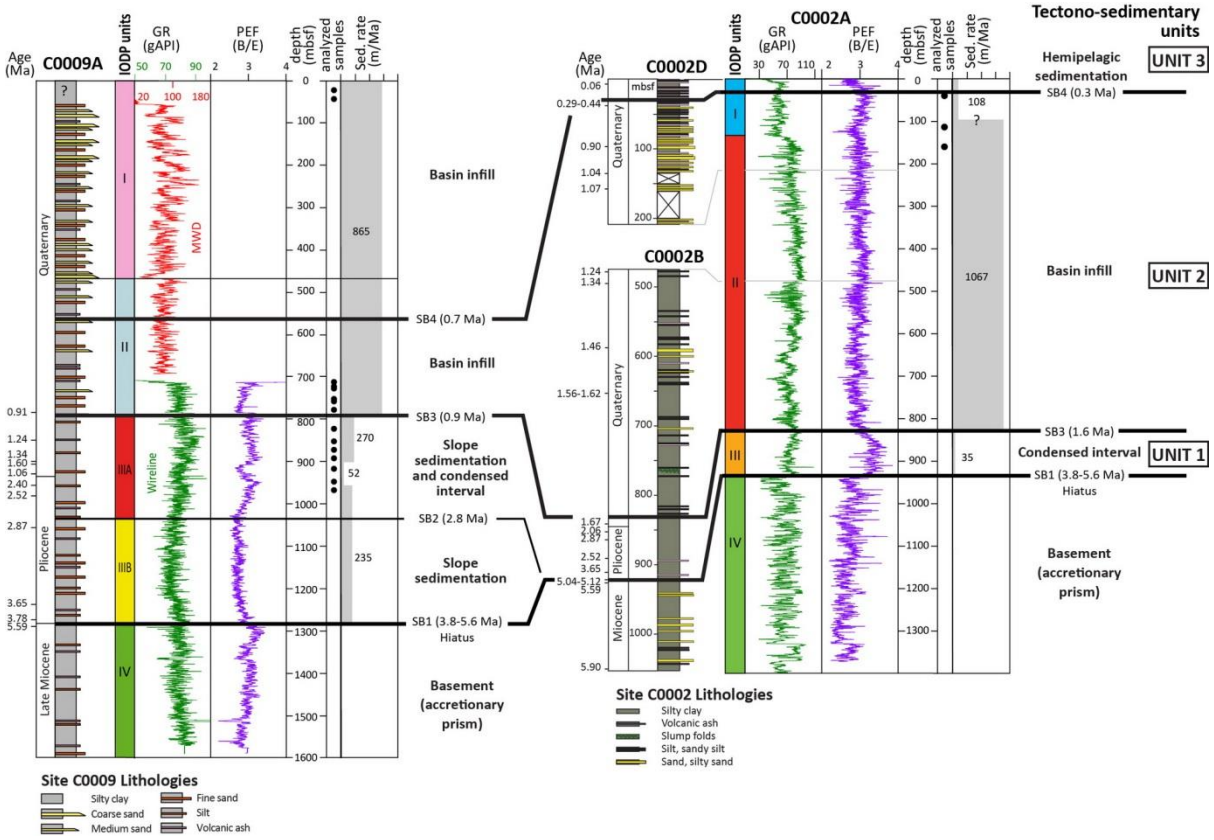

Corrected, unformatted version – full edited paper at http://doi.org/10.1016/j.epsl.2014.12.046

Figure 4. Seismic restoration showing geometrical evolution of the Kumano Basin during deposition of tectono-stratigraphic units.

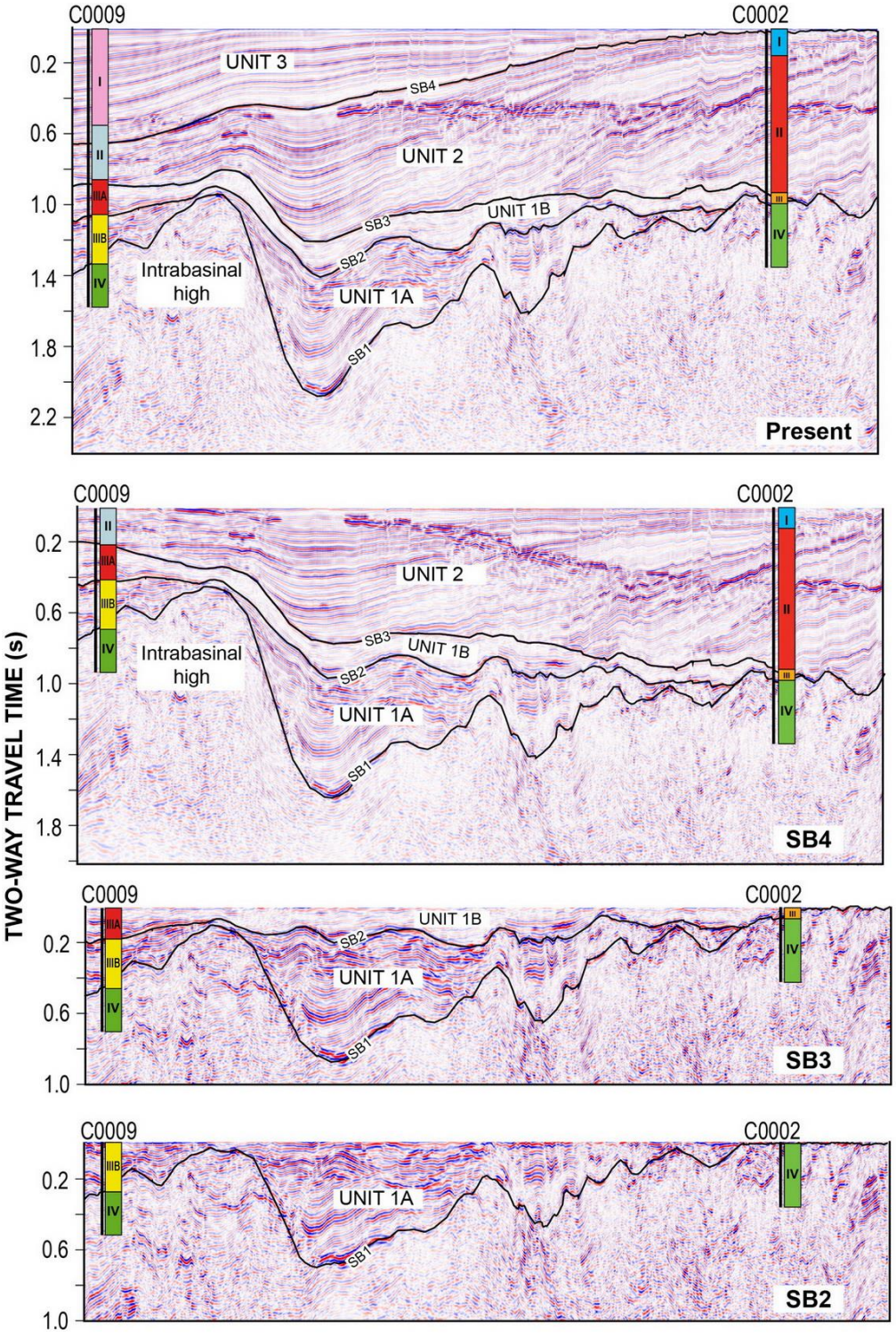

Figure 5. Tectonic discrimination diagrams of clinopyroxenes after Leterrier et al. (1982) applied to detrital pyroxenes from all sampled localities, including original density contours from Leterrier et al. (1982). Data expressed as cationic values from the structural formula of clinopyroxenes.

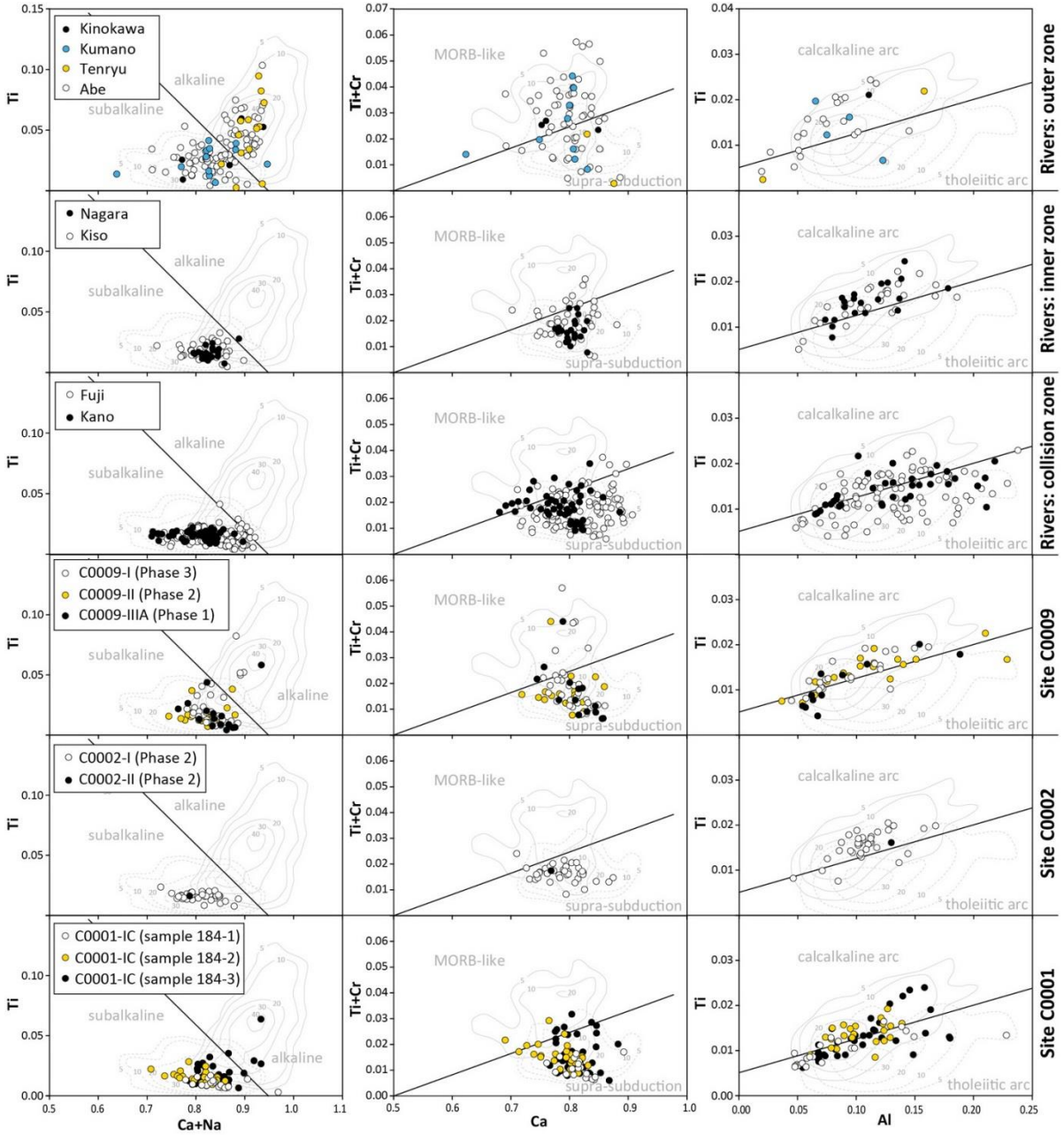

Corrected, unformatted version – full edited paper at http://doi.org/10.1016/j.epsl.2014.12.046

Figure 6. La/Sm vs Dy/Yb diagrams showing REE compositional variability of analysed detrital clinopyroxenes, with specific compositional spaces from Abe river and Inner Zone sources.

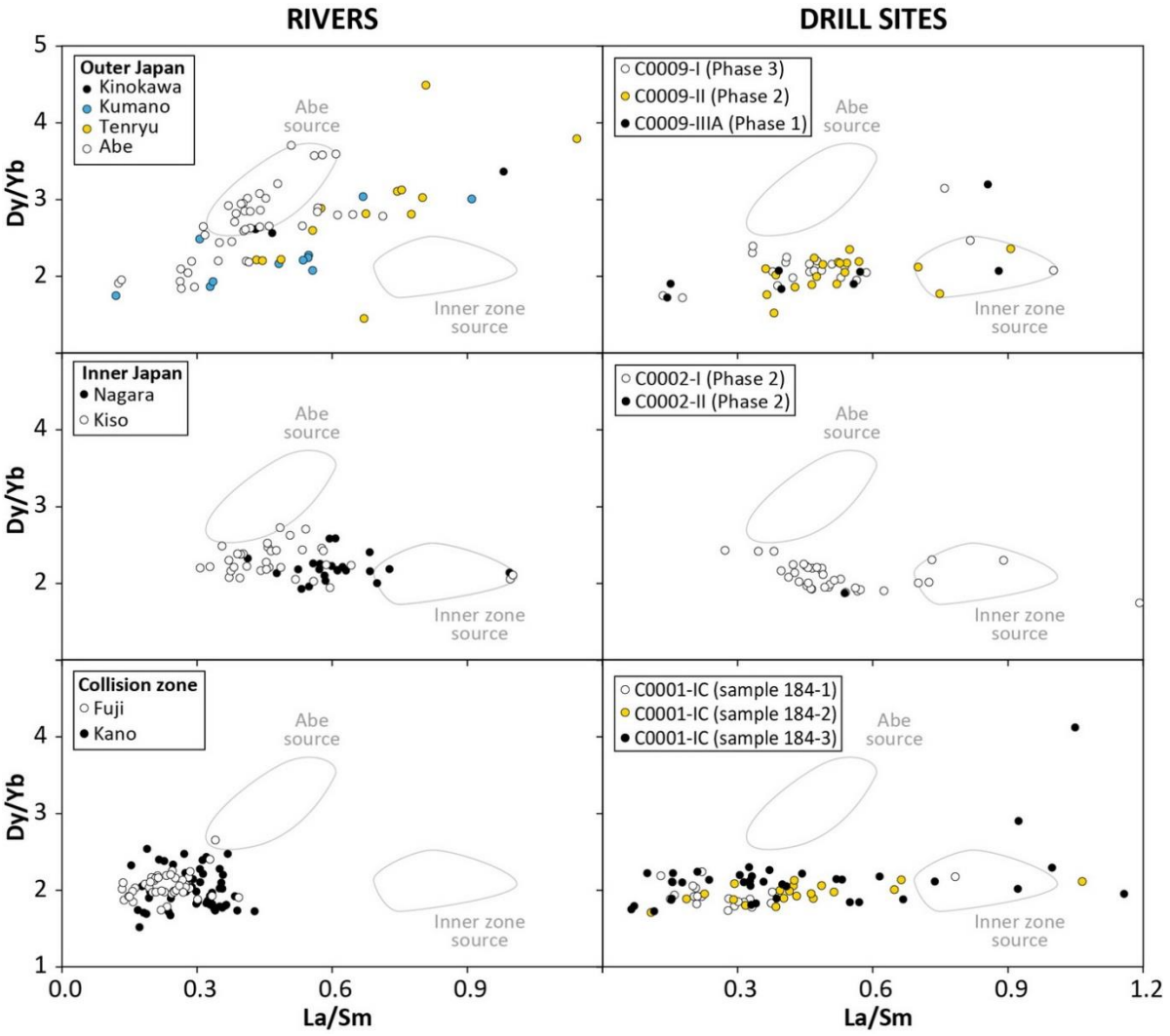

Corrected, unformatted version – full edited paper at http://doi.org/10.1016/j.epsl.2014.12.046

Figure 7. Compositional variability of detrital orthopyroxenes shown in %ferrosilite vs Al, Na and Ca diagrams, including specific compositional spaces from Kumano river, Tenryu river and Kano river sources. Data expressed as cationic values from the structural formula of orthopyroxenes.

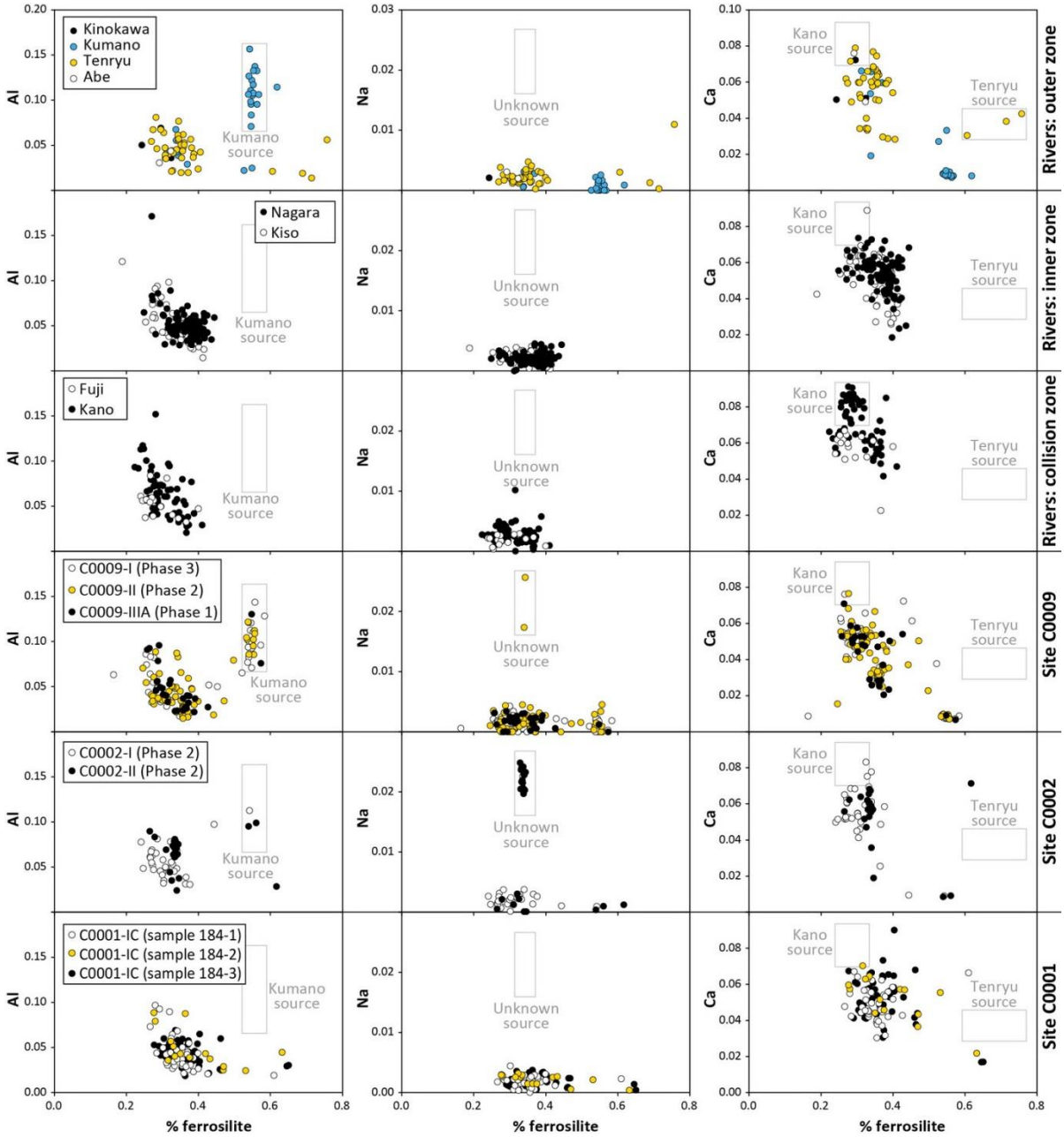

Corrected, unformatted version – full edited paper at http://doi.org/10.1016/j.epsl.2014.12.046

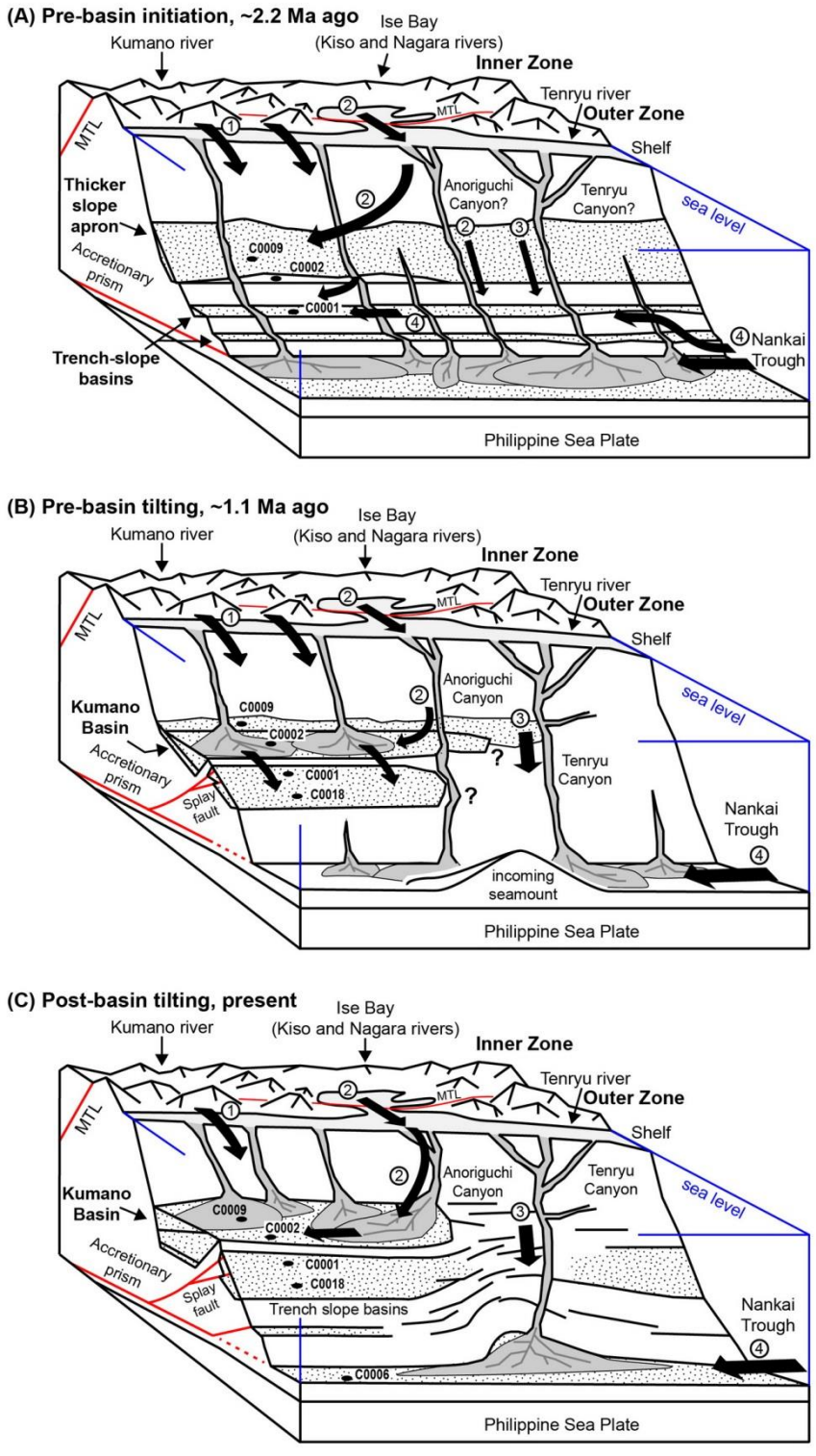

Figure 8. Summary diagram showing evolution of the Kumano Basin and nearby forearc area from (A) ~0.3 Ma before the basin initiation, to (B) early basin setting, and (C) present. Black arrows show sediment flow patterns determined based on the composition of detrital pyroxenes (1=Kumano river source, 2=Inner Zone source, 3=Tenryu river source, and 4=Collision Zone source). Important results include recognition of: (i) material from Collision Zone source at site C0001 ~2.2 Ma ago, which does not occur at other sampled drill sites during the Quaternary; and (ii) only limited longitudinal transport of sediments in the Kumano Basin, without supply from the Outer Zone further NE of the Ise Bay (e.g., Tenryu river source). MTL=Median Tectonic Line. Full explanation is given under Section 5.

Figure S1. Interpretation of sedimentation rates based on nannofossil ages (data from Kinoshita et al. 2008, Saffer et al. 2010 and Kameo and Jiang 2013**).**

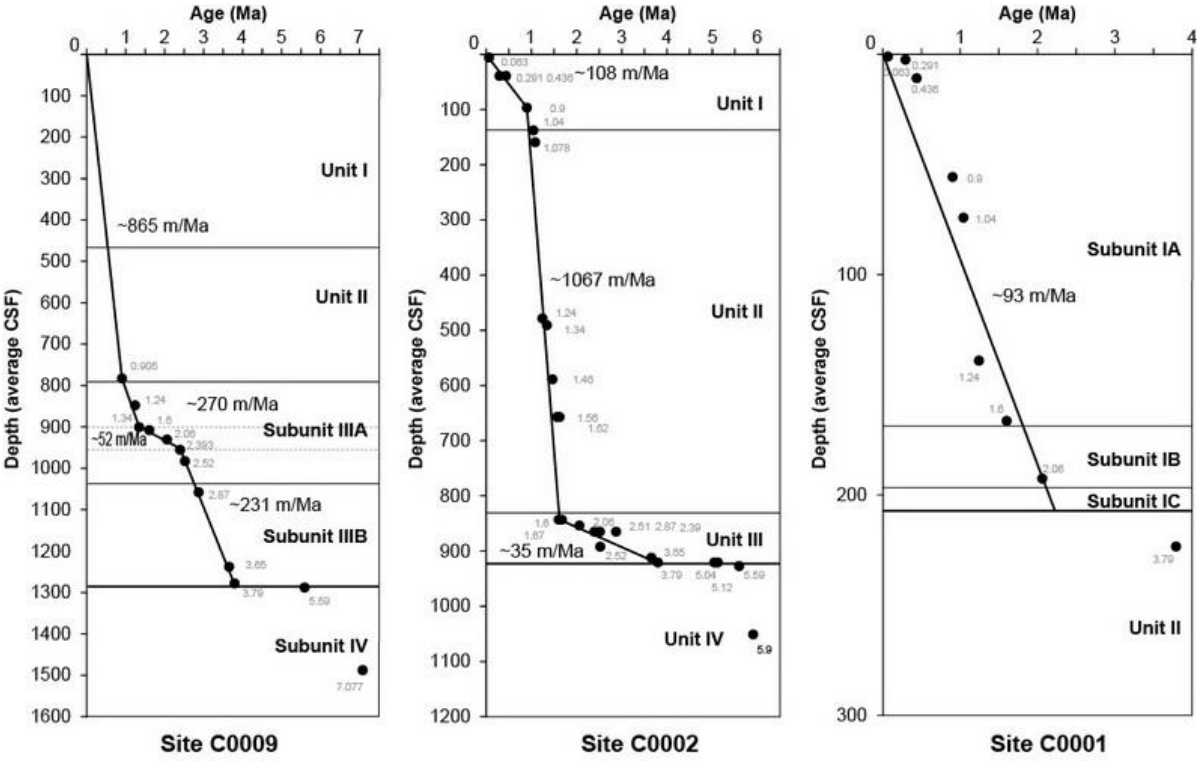

Corrected, unformatted version – full edited paper at http://doi.org/10.1016/j.epsl.2014.12.046

Figure S2. Simplified geological map showing the drainage systems of sampled rivers. Geology after Geological Survey of Japan (2012).

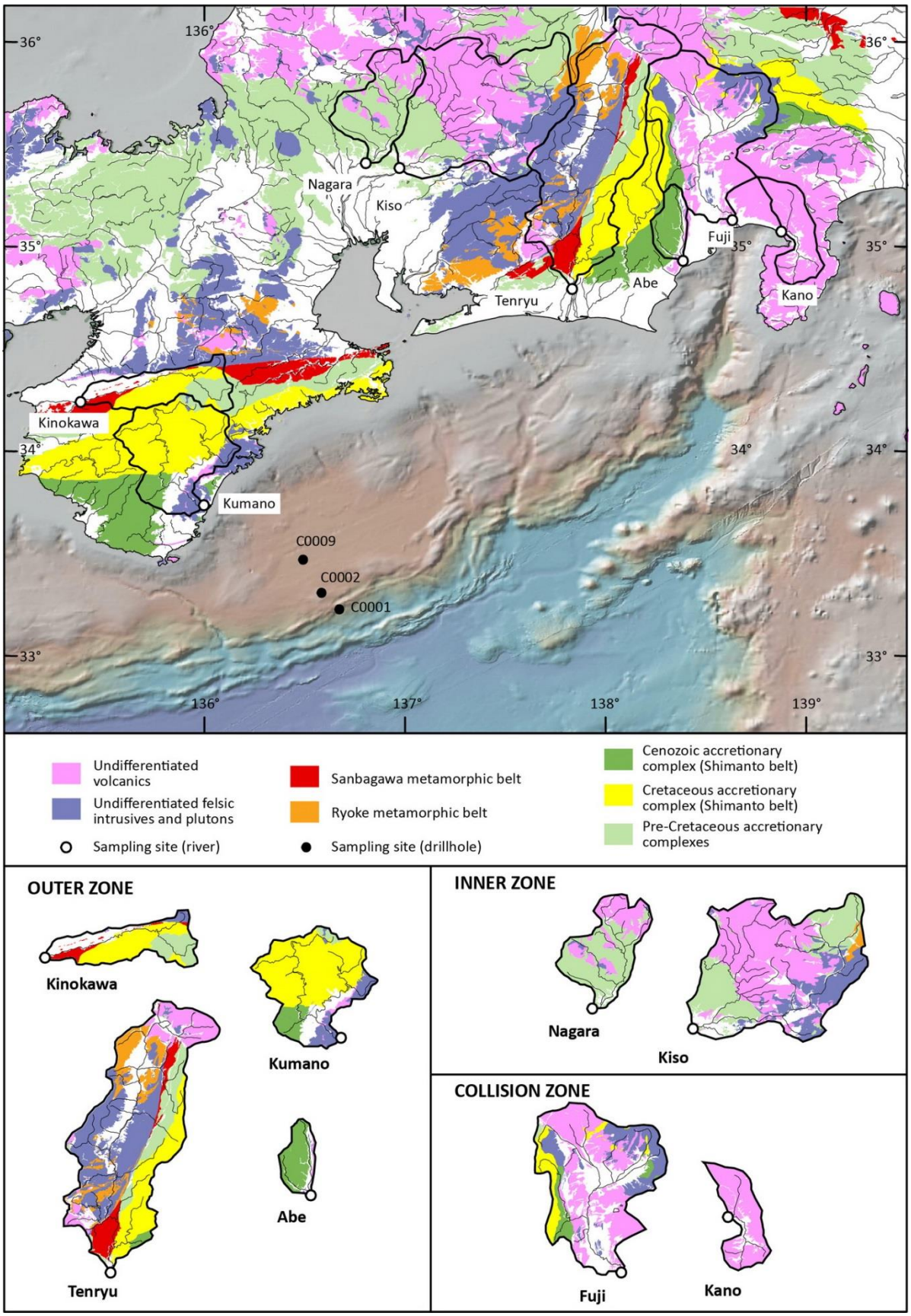

Corrected, unformatted version – full edited paper at http://doi.org/10.1016/j.epsl.2014.12.046

Figure S3. Classification diagram of pyroxenes displaying all analysed clinopyroxenes.

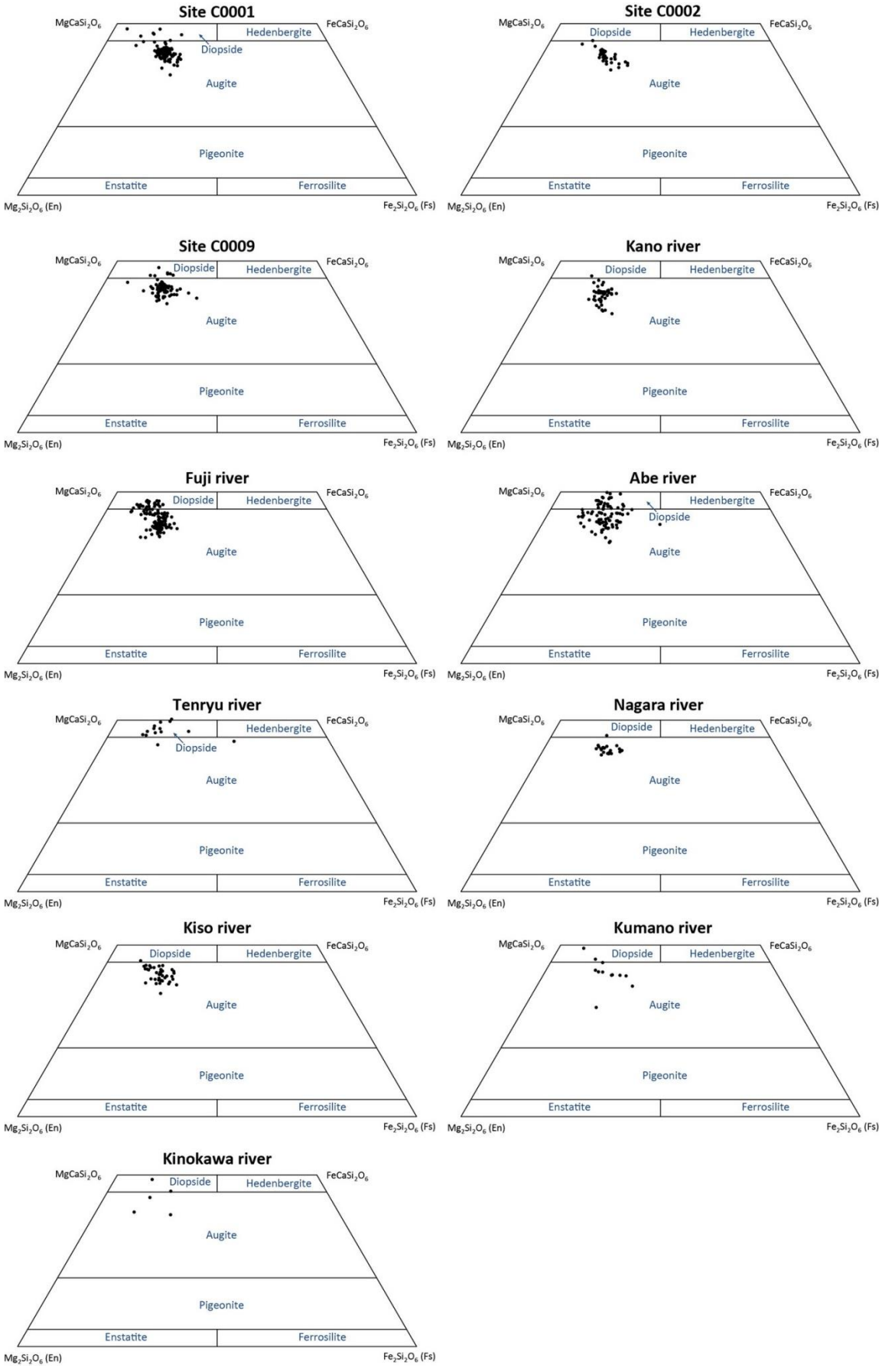

Corrected, unformatted version – full edited paper at http://doi.org/10.1016/j.epsl.2014.12.046

Figure S4. Reproducibility of Ti content in clinopyroxenes measured by microprobe and LA-ICP-MS techniques.

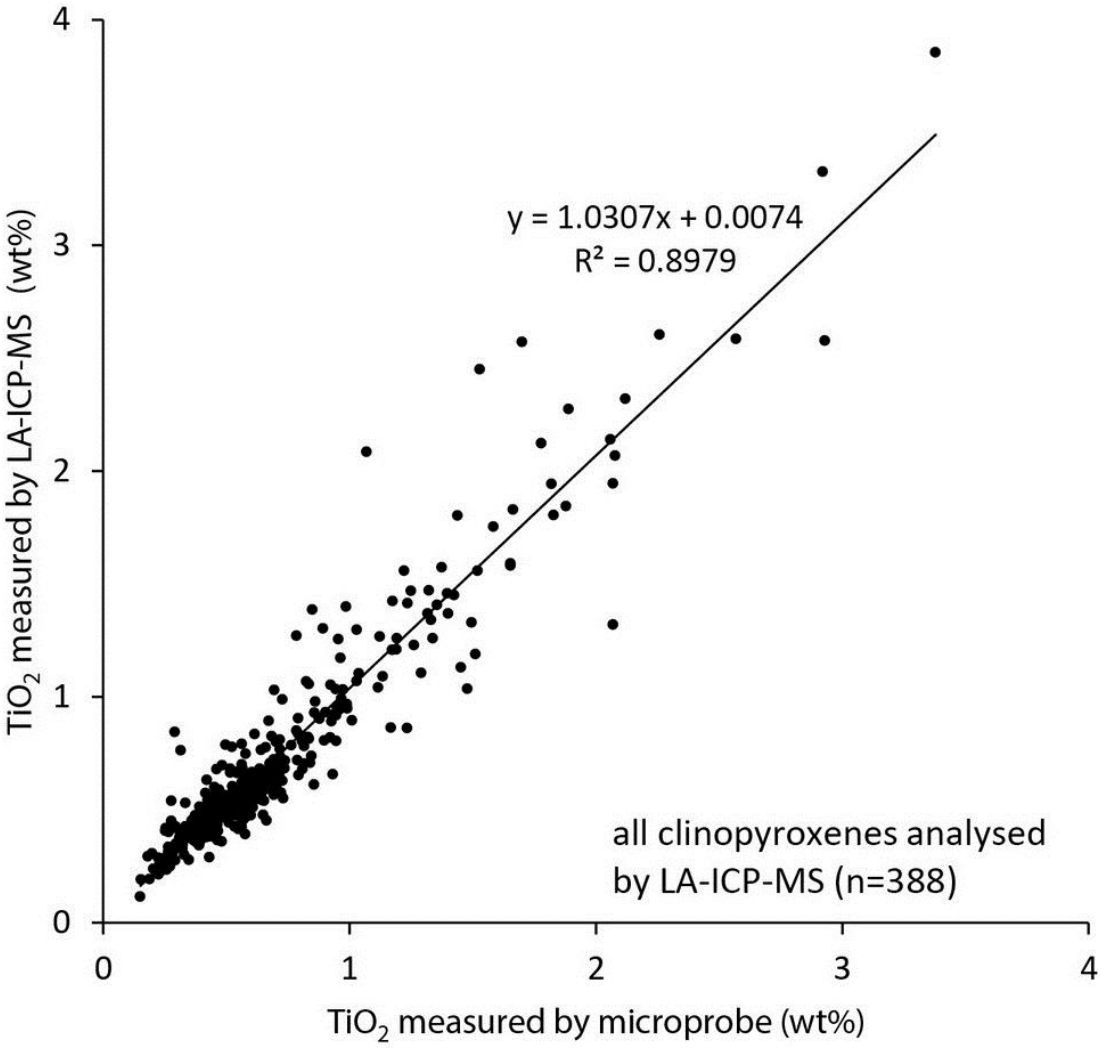

Corrected, unformatted version – full edited paper at http://doi.org/10.1016/j.epsl.2014.12.046

Table T1. List of samples with geographic and stratigraphic location. The number of analysed pyroxenes is given for each sample. **– available upon request or on http://doi.org/10.1016/j.epsl.2014.12.046**

Table T2. Pyroxene composition determined by microprobe analysis. **– available upon request or on http://doi.org/10.1016/j.epsl.2014.12.046**

Table T3. REE and Ti element contents of clinopyroxenes determined by LA-ICP-MS analysis. **– available upon request or on http://doi.org/10.1016/j.epsl.2014.12.046**

APPENDIX A - Stratigraphic accuracy of cuttings samples in IODP Hole C0009A

IODP Expedition 319 (drilling vessel Chikyu, NanTroSEIZE project) was the first to use a riser drilling system for scientific research applications. The riser drilling system permits deep drilling, retrieval of cuttings samples with quick assessment of lithostratigraphic changes downhole compared to traditional core recovery techniques. However, the study of cuttings samples may be affected by recovery processes leading to possible stratigraphic bias. Although cuttings samples have been used extensively in the industry, we have no knowledge of peer-reviewed contribution on their stratigraphic accuracy. Therefore, we combine below some observations made during Expedition 319 (Saffer et al., 2010) with new personal data to determine the accuracy and potential limitations of cuttings samples used for our sediment provenance analysis.

A1. Riser system and operations in Hole C0009A

The riser system on the Chikyu uses an outer casing that surrounds the drill pipe to provide return-circulation of dense and viscous drilling fluid to maintain pressure balance within the borehole. The drilling fluid carries cuttings (i.e. disaggregated sediment, minerals or lithic fragments mostly liberated at drilling depth), which can be sampled on the drilling vessel. Stratigraphic information in cuttings samples may be affected by the occurrence of cavings that consist of material produced by disaggregation of uncased borehole walls above the drill bit. At Hole C0009A, riserless drilling and installation of casing were conducted down to ~700 mbsf (meter below sea floor). Riser drilling and collection of cuttings samples was made in every 5 meters interval between depths of ~700 and ~1510 mbsf (cuttings samples 1 to 173). Both cuttings and cores were retrieved in the ~1510 to ~1600 mbsf interval (cuttings samples 176 to 193), before widening of the hole accompanied by sampling of new cuttings in the same depth interval (cuttings samples 196 to 215). Cuttings samples in Hole C0009A contain disaggregated sediment until ~1040 mbsf (boundary of Subunits IIIA and IIIB), and disaggregated sandy sediment plus poorly to well consolidated muddy sediment below this depth. Drilling of Hole C0009A was followed by wireline logging below ~700 mbsf that offers a stratigraphically accurate measurement of lithologic changes downhole (Saffer et al., 2010). Below we compare the composition of the cuttings and cores as well as logging data to characterize caving effects in Hole C0009A and potential mixing of detrital grains during retrieval.

A1. Stratigraphic accuracy of cuttings samples in Hole C0009A

As shown previously in Saffer et al. (2010), there is generally a good correlation between compositional changes of cuttings samples and the downhole variation of logging data (Fig. A1). The correlation is particularly clear at the transition from Subunit IIIB (slope sediments) to Unit IV (accretionary complex). High abundance of plant fragments in Subunit IIIB compared to Subunit IIIA (slope sediments) and Unit IV results in a sharp increase downhole of the "Wood Index" (i.e., qualitative assessment of the abundance of plant fragments by visual inspection) at the boundary of subunits IIIA and IIIB. This is in good agreement with the first occurrence, or drastic increase downhole of a particular grain species. However, we point out that the Wood Index remains high until ~40 m below Subunit IIIB - Unit IV boundary, suggesting persistent sampling of Subunit IIIB at least until this depth. This persistent sampling is also suggested by gradual changes of the composition of cuttings samples determined by shipboard XRF and XRD measurements across Subunit IIIB - Unit IV boundary. Comparison of silty mudstone in cuttings samples and cores are in good agreement, with exception of CaO or calcite

contents previously attributed to contamination of cuttings samples by drill mud (Saffer et al., 2010). Sandy layers observed in the cores were poorly consolidated. Therefore, compositional scattering of core samples relative to cuttings samples can be attributed to disaggregation of more sandy or silty sediments during the retrieval of cuttings, whereas these sediments could be collected and analyzed in the cores. Importantly, sediment disaggregation during retrieval is of no consequence on our sediment provenance analysis that is based on heavy mineral compositions. Shipboard data suggest, however, that disaggregation of sandier layers can promote inheritance of detrital grains up to ~40 m above the drilling depth.

To further characterize the accuracy of the depth interval associated with cuttings samples, we performed grain counting in a selection of cuttings samples at core depth. Our observations focused mainly on the 1567.7 to 1592.7 mbsf interval, where an increased abundance of tuff interbeds is documented in the cores between 1579.5 and 1582.3 mbsf, which can be used as a traceable stratigraphic horizon. Lithological characteristics of the cuttings were evaluated in ten samples retrieved during the coring phase (cuttings samples 189-193) and widening of the hole (cuttings samples 208-212) for three grain size fractions (1-4 mm, 0.25-1 mm and 0.045-0.25 mm), focusing on the abundance of tuff or glass fragments (Figs. A2 and A3). The larger size fractions are composed of fragments of sediment not disaggregated during drilling, whereas the smallest size fraction is composed of disaggregated sediment. Results show for all size fractions that cuttings recovered during the two drilling phases are compositionally distinct. Cuttings recovered during coring lack coarse grained, less consolidated lithologies and larger size fractions do not allow recognition of a tuff-rich horizon at ~1580 mbsf depth due to probable disaggregation of tuff lithologies during retrieval. In contrast, cuttings recovered during widening of the hole successfully document the occurrence of a tuff-rich interval, but the increase in tuff abundance occurs below the depth of the tuff horizon seen in the cores, and extends to several samples (i.e. 211 and 212). These observations suggest existence of a ~5 m error in the cuttings depth. Importantly, small size fractions recovered during the riser drilling phase (similar to mineral separates used in our study) successfully allow recognition of a tuff-rich horizon at core depth.

A3. Conclusions

Combination of existing and new data from Site C0009 in the Kumano basin shows that: (1) cuttings samples provide important insights into the nature of drilled formations, in particular with the first apparition or marked increase of the abundance downhole of specific lithological components; (2) stratigraphic accuracy of cuttings samples in Hole C0009A is ±5 m; and, (3) caving effects up to ~40 m above the drilling depth may be noticeable in some cuttings samples, but caving decreases uphole from the drill bit, therefore compositional bias in sediment provenance analyses is very limited at a ~50 m interval. Overall, these conclusions support our use of cuttings samples from Hole C0009A to reconstruct compositional changes at the scale of lithological units in the Kumano basin.

References

Saffer, D., McNeill, L., Byrne, T., Araki, E., Toczko, S., Eguchi, N., Takahashi, K., and the Expedition 319 Scientists, 2010. Proc. IODP, 319: Tokyo (Integrated Ocean Drilling Program Management International, Inc.). doi:10.2204/iodp.proc.319.2010

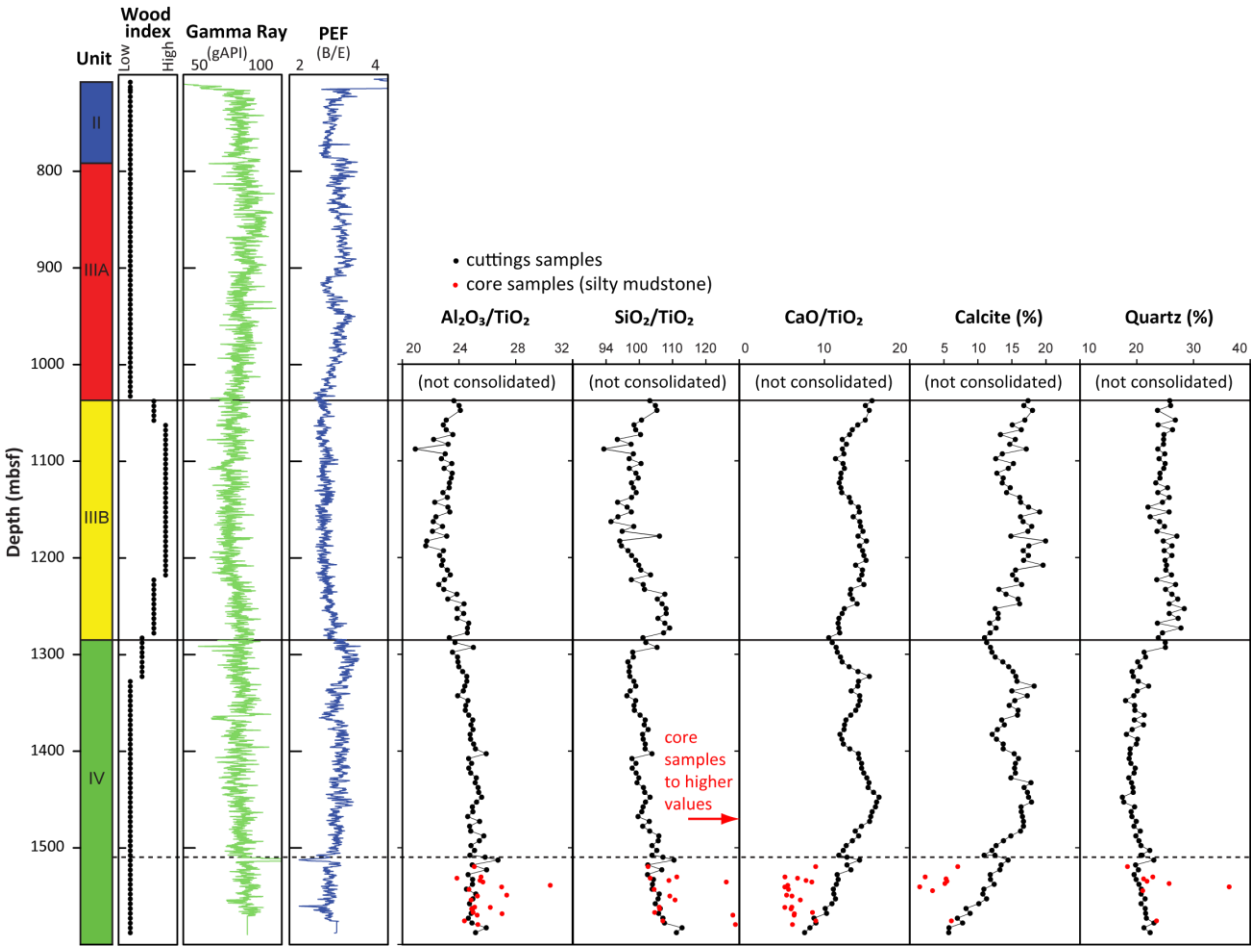

Figure A1. Selected compositional parameters of cuttings samples, cores and logging data in Hole C0009A (data after Saffer et al., 2010). The Wood Index represents qualitative assessment of the abundance of plant fragments by visual inspection. $Al_2O_3/TiO2$, SiO_2/TiO_2, CaO/TiO_2 ratios are based on shipboard XRF measurements of silty mudstone. Calcite and Quartz % are based on XRD shipboard measurements of similar sediment. Dashed line outlines starting depth of coring.

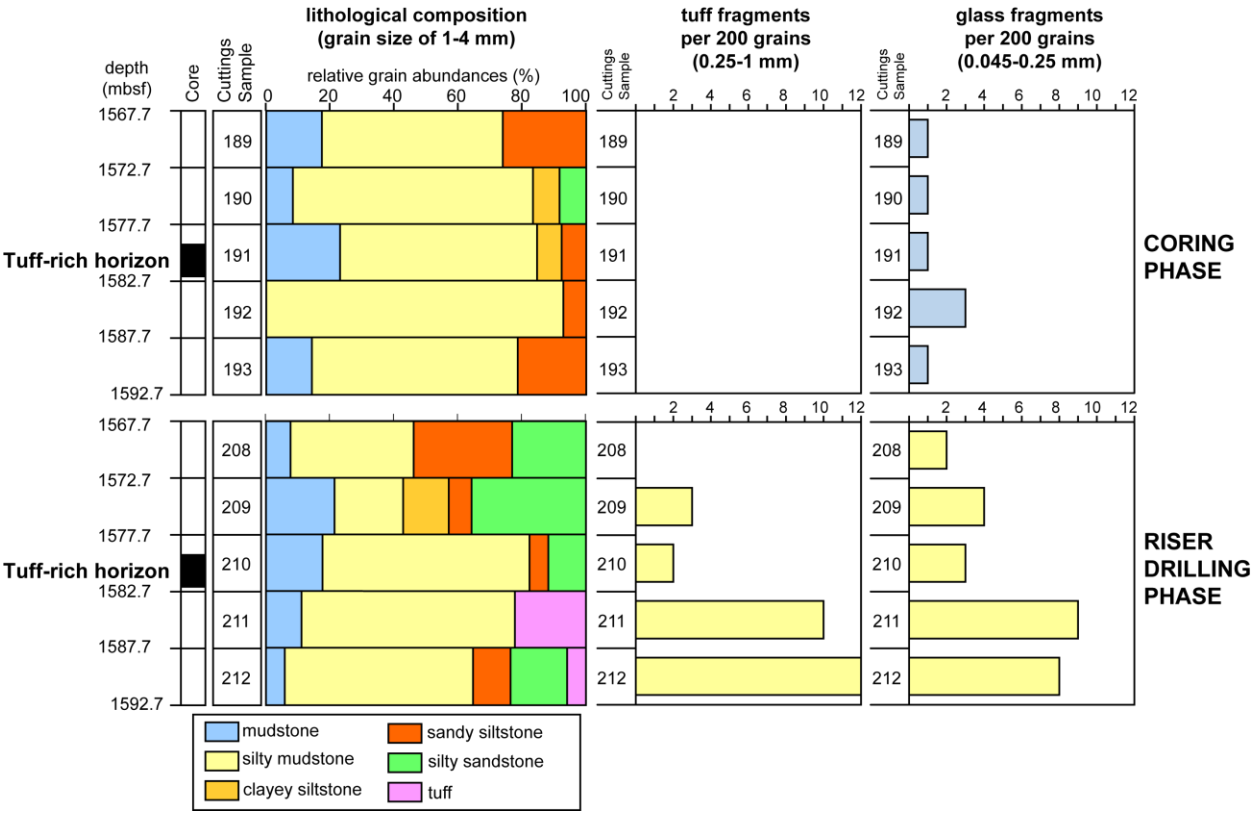

Figure A2. Results of grain counting in a selected interval at core depth. Lithological composition of 1-4 mm-sized cuttings were determined based on grain counting in thin sections (lithologies are illustrated in Fig. A4). Abundances of volcanic glass or tuff fragments were determined by grain counting in cuttings samples (grain size fractions 0.045-0.25 and 0.25-1 mm).

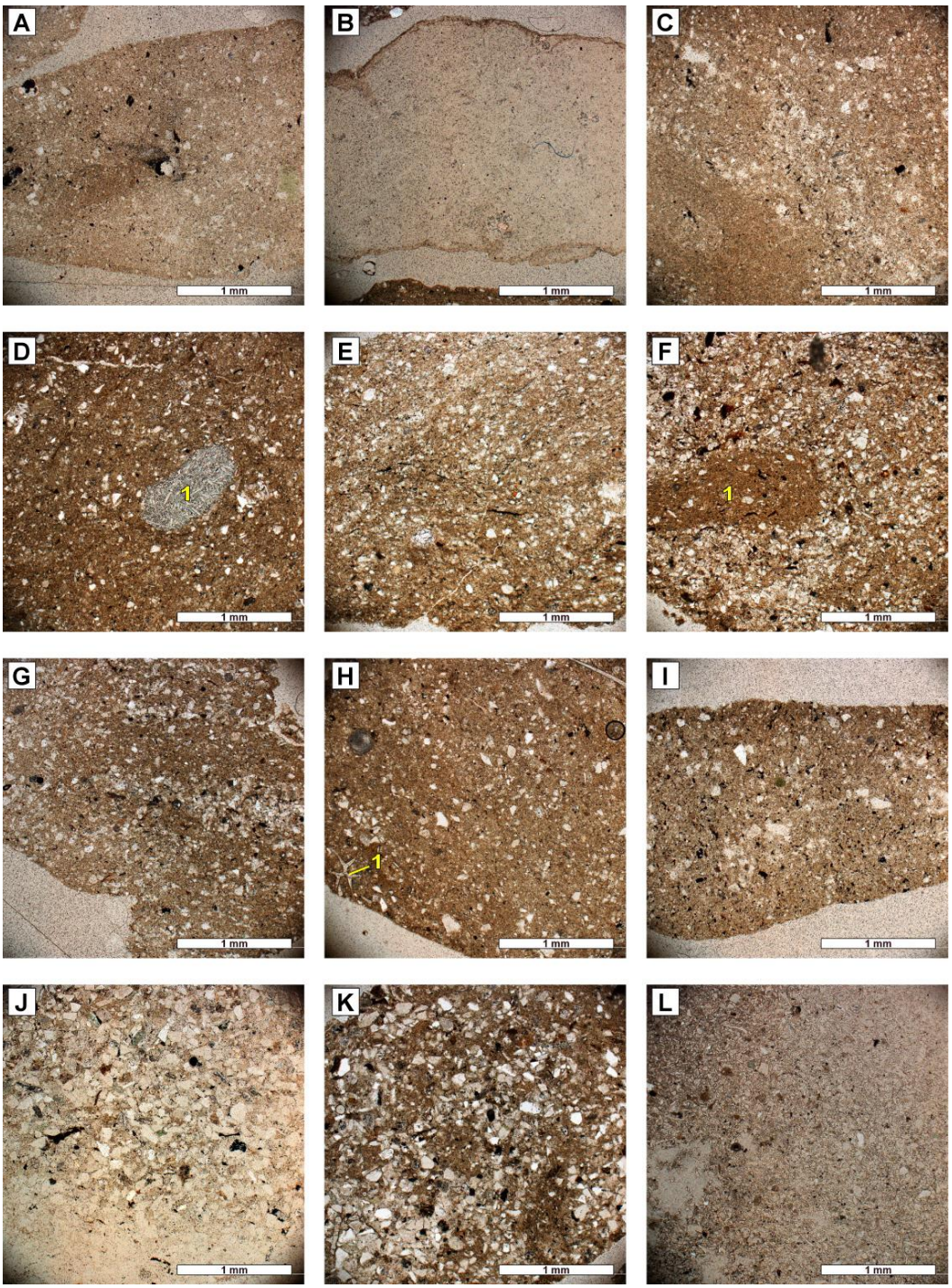

Figure A3. Typical lithologies of larger cuttings sampled during Exp. 319. A) mudstone (sample 319-C0009A-210SMW). B) Mudstone (sample 319-C0009A-210SMW). C) Mudstone (sample 319-C0009A-189SMW). D) Silty mudstone (sample 319-C0009A-190SMW), with biogenic tube filled by spicules (1). E) Silty mudstone (sample 319-C0009A-189SMW). F) Clayey siltstone (sample 319-C0009A-191SMW), with biogenic tube filled by mud (1). G) Clayey siltstone (sample 319-C0009A-190SMW). H) Sandy siltstone (sample 319-C0009A-208SMW), with well-preserved sponge spicules (1). I) Sandy siltstone (sample 319-C0009A-189SMW). J) Silty sandstone (sample 319-C0009A-209SMW). K) Silty sandstone (sample 319-C0009A-190SMW). L) Tuff (sample 319-C0009A-211SMW).

APPENDIX B - Analytical procedure

B1. Electron microprobe analysis

Most pyroxenes were analyzed using JEOL JXA 8200 electron microprobe equipped with 5 wavelength dispersive spectrometers including 3 high-sensitivity ones (2 PETH and TAPH) at the GEOMAR (Helmholtz Centre for Ocean Research Kiel). The analytical conditions were 15 kV accelerating voltage, 2 nA current and 1 μm electron beam size. Counting time was 20/10 s (peak/background) for Na, Ni, Mn, K, Si, Mg, Al, Ca, Ti, and 30/15s for Fe. Kakanui Augite (USNM 122142) for Si, Ti, Al, Fe, Mn, Mg, Ca, Na, New County Nevada Cr-Augite (NMNH 144905) for Cr, both from the Smithosonian collection of natural reference materials (Jarosevich et al., 1980), were used for calibration and monitoring of routine measurements. Two to three analyses of both standard pyroxenes were performed at the beginning of analytical session, after every 50-60 analyses and at the end. The data reduction included on-line CITZAF correction and small correction for systematic deviations (if any) from the reference values obtained on standard materials. The later correction did not exceed 5 % relative for all elements and allowed to achieve the best possible accuracy of the data and long-term reproducibility.

Some pyroxenes (specified in Table T2) were analysed using wavelength dispersion spectrum (WDS) type electron microprobe JEOL-8800 at the Department of Earth and Planetary Sciences, Tokyo Institute of Technology. Analytical conditions were 12 nA of current and 15 kV of accelerating voltage, and the beam was focused < 2 μm of diameter. Unless being noted specifically, composition of minerals was analysed at one point at the centre for each grain. Analytical results were corrected by ZAF method.

The structural formula of pyroxenes was calculated using the method given in Morimoto et al. (1988).

B2. LA-ICP-MS analysis

In total, 388 clinopyroxenes analyzed by electron microprobe at the GEOMAR were selected for analysis of 29 trace elements by laser ablation ICP-mass spectrometry (LA-ICP-MS) at Christian-Albrecht-Universität Kiel. A 193 nm ArF excimer laser ablation system (GeoLasPlus, Coherent) coupled to an Agilent 7500s ICP-MS was used for all measurements. Samples were loaded to a Zurich-type low dispersion high capacity laser ablation cell (LDHCLAC) flushed with 1.0 l·min-1 He as the carrier gas. Addition of 14 mL·min-1 H2 into the He carrier gas stream before entering the ablation cell led to an increase in sensitivity

and reduction of oxide formation (typically <0.2 % ThO/Th). For single spot ablation wit 50-80 µm crater size the laser was operated with 15Hz pulse frequency at a fluence of 10 J cm^{-2}. Any single measurement comprised data acquisition for 33 isotopes with 10ms dwell time in intervals of 20s background, 40s sample ablation, and 20s for washout monitoring. Further data processing was done using the GLITTER software package using the integrated graphical visualization tool for setting integration intervals for each analyzed spot. Background counts were used for calculating actual lower limits of detection. To reduce potential error introduced from both sample surface contamination and instable aerosol particle distribution during the first laser shots the first couple of seconds of each sample acquisition interval was discarded from data integration. Data being affected from inclusions of other minerals or melts were skipped from sample integration. In GLITTER external calibration was done with the silicate glass standard reference material NIST SRM612 using 48Ca for internal standardization and preferred values from Jochum et al. (2011). Data obtained this way with non-matrix matched NIST-glass calibration typically has a systematic bias of the results as a consequence of different sample matrices. Thus, a second matrix-matched calibration step using a series of vitrified rock SRMs (BIR-1G, BCR-2G: preferred values from GeoRem online data repository; MPI-DING-glasses StHs-6/80-G, GOR128-G, BM-90/21-G: preferred values from Jochum et al. [2006]) was applied using external spreadsheet software. From that SRM data an average "bias factor" was calculated for each element. NIST-glass calibrated sample data was then recalibrated applying these bias factors. The calculated bias factors were stable within <5% RSD over the entire duration of the 8 LA-ICP-MS sessions covering 3 months. All final data presented in the results tables are background corrected and represent averages of 1-4 replicates within each clinopyroxene crystal. Data for analyzed reference materials and replicate analyses are compiled in Table T4.

References

Jarosewich, E.J., Nelen, J.A., Norberg, J.A., 1980. Reference Samples for Electron Microprobe Analysis, Geostandards Newsletter 4, 43-47.

Jochum, K.P., Stoll, B., Herwig, K., Willbold, M., Hofmann, A.W., Amini, M., Aarburg, S., Abouchami, W., Hellebrand, E., Mocek, B., 2006. MPI‐DING reference glasses for in situ

microanalysis: New reference values for element concentrations and isotope ratios. Geochem Geophys Geosyst 7. doi:10.1029/2005GC001060

Jochum, K.P., Weis, U., Stoll, B., Kuzmin, D., Yang, Q., Raczek, I., Jacob, D.E., Stracke, A., Birbaum, K., Frick, D.A., Günther, D., Enzweiler, J., 2011. Determination of Reference Values for NIST SRM 610-617 Glasses Following ISO Guidelines. Geostandards and Geoanalytical Research 35, 397–429. doi:10.1111/j.1751-908X.2011.00120.x

Morimoto, N., Fabries, J., Ferguson, A.K., Ginzburg, I.V., Ross, M., Seifert, F.A., Zussman, J., Aoki, K., Gottardi, G., 1988. Nomenclature of pyroxenes. American Mineralogist 73, 1123-1133.